

Southern Illinois University Carbondale

OpenSIUC

---

Theses

Theses and Dissertations

---

5-1-2020

## EFFECT OF BUILDING ORIENTATION ON STRUCTURAL RESPONSE OF REINFORCED CONCRETE MOMENT RESISTING FRAME STRUCTURES

Amanullah Parsa

*Southern Illinois University Carbondale*, amanullah.parsa@siu.edu

Follow this and additional works at: <https://opensiuc.lib.siu.edu/theses>

---

### Recommended Citation

Parsa, Amanullah, "EFFECT OF BUILDING ORIENTATION ON STRUCTURAL RESPONSE OF REINFORCED CONCRETE MOMENT RESISTING FRAME STRUCTURES" (2020). *Theses*. 2698.

<https://opensiuc.lib.siu.edu/theses/2698>

This Open Access Thesis is brought to you for free and open access by the Theses and Dissertations at OpenSIUC. It has been accepted for inclusion in Theses by an authorized administrator of OpenSIUC. For more information, please contact [opensiuc@lib.siu.edu](mailto:opensiuc@lib.siu.edu).

EFFECT OF BUILDING ORIENTATION ON STRUCTURAL RESPONSE OF  
REINFORCED CONCRETE MOMENT RESISTING FRAME STRUCTURES

by

Amanullah Parsa

B.E., Osmania University, 2015

A Thesis

Submitted in Partial Fulfillment of the Requirements for the  
Master of Science Degree

Department of Civil and Environmental Engineering  
in the Graduate School  
Southern Illinois University Carbondale  
May 2020

Copyright by Amanullah Parsa, 2020  
All Rights Reserved

THESIS APPROVAL

EFFECT OF BUILDING ORIENTATION ON STRUCTURAL RESPONSE OF  
REINFORCED CONCRETE MOMENT RESISTING FRAME STRUCTURES

by

Amanullah Parsa

A Thesis Submitted in Partial  
Fulfillment of the Requirements  
for the Degree of  
Master of Science  
in the field of Civil Engineering

Approved by:

Dr. Jale Tezcan, Chair

Dr. Aslam Kassimali

Dr. J. Kent Hsiao

Graduate School  
Southern Illinois University Carbondale  
April 7, 2020

## AN ABSTRACT OF THE THESIS OF

Amanullah Parsa, for the Master of Science degree in Civil Engineering, presented on April 7, 2020, at Southern Illinois University Carbondale.

TITLE: EFFECT OF BUILDING ORIENTATION ON STRUCTURAL RESPONSE OF REINFORCED CONCRETE MOMENT RESISTING FRAME STRUCTURES.

MAJOR PROFESSOR: Dr. Jale Tezcan

In time history analysis of structures, the geometric mean of two orthogonal horizontal components of ground motion in the as-recorded direction of sensors, have been used as measure of ground motion intensity prior to the 2009 NEHRP provision. The 2009 NEHRP Provisions and accordingly the seismic design provisions of the ASCE/SEI 7-10, modified the definition of ground motion intensity measure from geometric mean to the maximum direction ground motion, corresponding to the direction that results in peak response of the oscillator. Maximum direction response spectra are assumed to envelope the range of maximum possible responses over all nonredundant rotation angles. Two assumptions are made in the use maximum ground motion as the intensity measure: (1) the structure's strength and stiffness properties are identical in all directions and (2) azimuth of the maximum spectral acceleration coincides with the one of the principal axes of the structure. The implications of these assumptions are examined in this study, using 3D computer models of multi-story structures having symmetric and asymmetric layouts and elastic vibration period of 0.2 second and 1.0 second subjected to a set of 25 ground-motion pairs recorded at a distance of more than 20 km from the fault. The influence of the ground-motion rotation angle on structural response (here lateral displacement and story drift) is examined to form benchmarks for evaluating the use of the maximum direction (MD) ground motions. The results of this study suggest that while MD ground motions do not always result in largest structural response, they tend to produce larger response than the as-recorded ground

motions. On the other hand, more research on non-linear seismic time history analysis is recommended, especially for asymmetric layout plan buildings.

## ACKNOWLEDGMENTS

I would like to express my deep gratitude to my academic advisor and my thesis committee chair Dr. Jale Tezcan for accepting me and her kind help and support through successful completion of my thesis work. I am grateful for her time spent on guiding and mentoring me during this research.

I would like to express my deep indebtedness to my committee members Dr. Aslam Kassimali and Dr. J. Kent Hsiao for providing valuable assistance, suggestions and comments on this research. I am proud to attend the classes taught by such great professors to expand my knowledge of Structural Engineering.

I am grateful to Head of Civil and Environmental Engineering Department, Dr. Sanjeev Kumar, faculty, staff and students of Southern Illinois University Carbondale for their help and support throughout my master's degree program.

I am thankful to the United States government and people for providing me the Fulbright Scholarship to study my Master of Science degree in the U.S. which was a dream to me.

My special thanks go to my lovely family in my home country Afghanistan, my parents, my wife Nazifa Parsa, my lovely son Emran Parsa, my brothers and my sister for their love and support during my graduate program.

## TABLE OF CONTENTS

| <u>CHAPTER</u>                              | <u>PAGE</u> |
|---|-------------|
| ABSTRACT.....                               | i           |
| ACKNOWLEDGMENTS .....                       | iii         |
| LIST OF TABLES .....                        | vi          |
| LIST OF FIGURES .....                       | vii         |
| CHAPTERS                                    |             |
| CHAPTER 1 INTRODUCTION .....                | 1           |
| 1.1 STATEMENT OF THE PROBLEM.....           | 2           |
| 1.2 SCOPE OF THE RESEARCH .....             | 5           |
| 1.3 ORGANIZATION OF THESIS .....            | 6           |
| CHAPTER 2 LITERATURE REVIEW .....           | 8           |
| 2.1 GEOMETRIC MEAN OF GROUND MOTIONS.....   | 8           |
| 2.2 ROTATION OF GROUND MOTIONS.....         | 8           |
| 2.3 MAXIMUM DIRECTION GROUND MOTIONS .....  | 9           |
| CHAPTER 3 METHODOLOGY AND APPLICATION ..... | 15          |
| 3.1 INTRODUCTION .....                      | 15          |
| 3.2 GROUND MOTIONS SELECTED (DATA) .....    | 15          |
| 3.3 STAAD PRO .....                         | 20          |
| 3.4 BUILDING MODELS.....                    | 20          |
| 3.5 TIME HISTORY ANALYSIS.....              | 24          |
| CHAPTER 4 RESULTS AND DISCUSSION.....       | 25          |
| 4.1 RESULTS .....                           | 25          |



|   |    |
|---|----|
| 4.2 LATERAL DISPLACEMENT .....  | 25 |
| 4.3 STORY DRIFT .....   | 26 |
| 4.4 DISCUSSION .....  | 47 |
| CHAPTER 5 CONCLUSION AND RECOMMENDATIONS .....  | 49 |
| 5.1 RECOMMENDATIONS .....   | 50 |
| REFERENCES .....  | 51 |
| APPENDICES  |    |
| APPENDIX A – TIME HISTORY ANALYSIS RESULT .....   | 53 |
| APPENDIX B – MAXIMUM ROOF DISPLACEMENT UNDER AS-RECORDED<br>AND MD GROUND MOTIONS ..... | 67 |
| VITA .....  | 70 |

LIST OF TABLES

| <u>TABLE</u>  | <u>PAGE</u> |
|---|-------------|
| Table 1 - Selected ground motion records .....                                    | 17          |
| Table 2 - Maximum roof displacement under as-recorded and MD ground motions. .... | 68          |

## LIST OF FIGURES

| <u>FIGURE</u>   | <u>PAGE</u> |
|---|-------------|
| Figure 1 - Trace of pseudo acceleration of single lumped mass oscillator.....   | 4           |
| Figure 2 - Distribution of magnitude ( $M_w$ ) and fault distance ( $R_{rup}$ ) for the 25-ground motion records selected.....  | 18          |
| Figure 3 - Response spectra of 25 ground motion records selected .....  | 18          |
| Figure 4 - Polar plots of spectral acceleration values with respect to rotation angles ( $\theta_x$ ).....  | 19          |
| Figure 5 - Plan view of BM1 and BM3 .....   | 21          |
| Figure 6 - Plan view of BM2 and BM4 .....   | 22          |
| Figure 7 - 3D view of BM1.....  | 22          |
| Figure 8 - 3D view of BM2.....  | 23          |
| Figure 9 - 3D view of BM3.....  | 23          |
| Figure 10 - 3D view of BM4.....   | 24          |
| Figure 11 - Variation of lateral displacement (cm) at roof level ( $U_x$ ) in the X-direction of BM1 as a function of the rotation angle, $\theta_x$ subjected to (GM1-25)..... | 27          |
| Figure 12 - Variation of lateral displacement (cm) at roof level ( $U_z$ ) in the Z-direction of BM1 as a function of the rotation angle, $\theta_x$ subjected to (GM1-25)..... | 29          |
| Figure 13 - Variation of lateral displacement (cm) at roof level ( $U_x$ ) in the X-direction of BM2 as a function of the rotation angle, $\theta_x$ subjected to (GM1-25)..... | 31          |
| Figure 14 - Variation of lateral displacement (cm) at roof level ( $U_z$ ) in the Z-direction of BM2 as a function of the rotation angle, $\theta_x$ subjected to (GM1-25)..... | 33          |
| Figure 15 - Variation of lateral displacement (cm) at roof level ( $U_x$ ) in the X-direction of BM3 as a function of the rotation angle, $\theta_x$ subjected to (GM1-25)..... | 35          |

Figure 16 - Variation of lateral displacement (cm) at roof level ( $U_z$ ) in the Z-direction of BM3 as a function of the rotation angle,  $\theta_x$  subjected to (GM1-25).....37

Figure 17 - Variation of lateral displacement (cm) at roof level ( $U_x$ ) in the X-direction of BM4 as a function of the rotation angle,  $\theta_x$  subjected to (GM1-25).....39

Figure 18 - Variation of lateral displacement (cm) at roof level ( $U_z$ ) in the Z-direction of BM4 as a function of the rotation angle,  $\theta_x$  subjected to (GM1-25).....41

Figure 19 - Story drift variation in the X-direction at center of mass as a function of rotation angle  $\theta_x$ , for BM1 subjected to (GM21, GM16, GM2) .....43

Figure 20 - Story drift variation in the X-direction at center of mass as a function of rotation angle  $\theta_x$ , for the BM2 subjected to (GM21, GM16, GM2).....43

Figure 21 - Story drift variation in the X-direction at center of mass as a function of rotation angle  $\theta_x$ , for the BM3 subjected to (GM21, GM16, GM2).....44

Figure 22 - Story drift variation in the X and Z direction at center of mass as a function of rotation angle  $\theta_x$ , for BM3 subjected to (GM16).....45

Figure 23 - Story drift variation in the X-direction at center of mass (cm) as a function of rotation angle  $\theta_x$ , for BM4 subjected to (GM21, GM16, GM2) .....46

# CHAPTER 1

## INTRODUCTION

Earthquake ground motion accelerations are recorded by triaxial accelerographs with accelerations in two horizontal component and one vertical component. The seismic design of many structures requires at least two horizontal ground motion components or all three components for the time history analysis of 3-dimensional structures, in which the structural response is computed considering those two or three components. Directionality of two horizontal components of ground motion relative to the principal axes of the structure is critical for calculation of structural response. For instance, a slight change in the building orientation (alternatively rotating the ground motion components) may change the value of structural response significantly. Considering the significant effect of building orientation on the structural response, there is not enough guidance in the design codes proposing a specific direction which the two horizontal components of ground motion should be applied to the structure.

New measures of ground motion intensity in ASCE 7-10 standard, which proposes maximum direction (MD) rather than geometric mean (GM), has drawn attentions to challenges in defining intensity measures and its implications on selecting, scaling, response evaluation and interpretation of the response. As the maximum direction ground motion does not necessarily coincide with a principal axis of the structure, the suitability of maximum direction ground motion as an appropriate ground motions intensity measure has been questioned. Furthermore, the effect of maximum direction intensity measure on the design of eccentric structures (having asymmetric plan) which are subjected to torsion during earthquakes, is unclear.

This thesis aims to investigate the effect of building orientation on the structural response of reinforced concrete moment resisting frame structure. For ease of operation, the horizontal

pair of ground motions has been rotated instead of rotating the building. Four different building models and a group of 25 ground motions pairs has been selected for this purpose. The building models includes symmetric and asymmetric layout plans. The group of 25 ground motions pairs are rotated through all non-redundant rotation angles and then applied to the building models in terms of seismic time history load to the building's principal directions (here X and Z axes of structure), and then the response of the structures has been recorded with respect to the rotation angle in terms of lateral displacement and story drift at center of mass of the floor level.

### **1.1 STATEMENT OF THE PROBLEM**

The ground motions intensity measures are primarily focused on two orthogonal components of horizontal ground motion, while the component orientation is arbitrary, depending on the orientation of the sensors. The two horizontal components of ground motion are needed for the response history analysis of structures, according to seismic design codes. Most seismic design codes used geometric mean of the two orthogonal components of horizontal ground motions ( $Sa_{GM}$ ) for response history analysis of structures, ahead of the Next Generation Attenuation (NGA) project (Power et. al, 2008).

The geometric mean of the two horizontal ground motion components was mostly favored because, it lowers the scattering of data and approximates the central value of casually oriented horizontal ground motion components. Geometric mean of the spectral accelerations of the two horizontal ground motion components for a fixed damping ratio, the geometric mean in 'X' and 'Y' direction (here termed as  $Sa_x$  and  $Sa_y$ ) are obtained as follows:

$$Sa_{GM}(T) = \sqrt{Sa_x(T) \times Sa_y(T)} \quad (1)$$

Where T is the vibration period.

However, the amplitudes of ground motion components are not the same at all rotation

angles in the geometric mean of ground motions intensity measure. It means that the actual ground motion intensity measure in the desired rotation angle could be different from the recorded orientation of ground motion components.

The NEHRP 2009 (National Earthquake Hazards Reduction Program) Seismic Provisions, modified the definition of horizontal ground motion intensity measure from the geometric mean of ground motions to the maximum direction ground motions. The maximum direction (MD) ground motion is in the direction which results in the maximum response of an oscillator considering all non-redundant rotation angles. As the maximum motion changes with the period of oscillator, the amplitude of maximum direction spectral pseudo-acceleration can vary at each period. The maximum direction ground motion at a desired period can be obtained by rotating the two given pairs of ground motion through all non-redundant rotations angles and taking out the maximum pseudo-acceleration for that period. Alternatively, we can obtain the maximum direction ground motion for a desired period graphically by plotting the pseudo-acceleration trace of a linear oscillator subjected to the pair of horizontal ground motion components and locating the point furthest away from the origin. Figure 1 illustrates an example using the 1956 El Alamo Earthquake recording from El Centro Array# 9 Station for an oscillator with vibration period  $T= 1.0$  second and damping ratio  $\zeta= 5\%$  , red line shows the direction and magnitude of the maximum pseudo-acceleration of the oscillator, defining the MD spectral ordinate at  $T=1$  second.

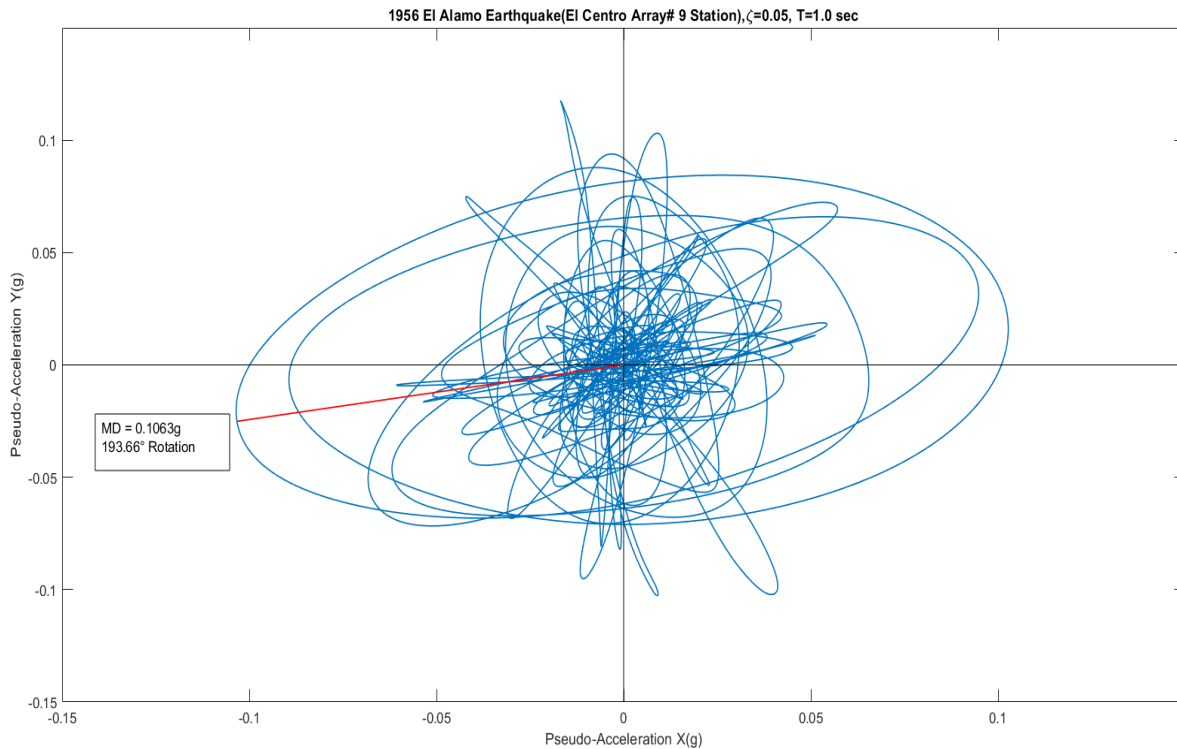


**Figure 1.** Trace of pseudo acceleration of a linear oscillator. The red line represents the magnitude and direction of maximum pseudo-acceleration.

As opposed to the NGA project using GMRotI50, the maximum direction is not a geometric mean measure of ground motions. Hence, the 2009 NEHRP Provision maps used the maximum direction to geometric mean ratios of 1.1 and 1.3 for short and mid-periods respectively (from Huang et al. 2008) to transform from the geometric mean maps. Accordingly, the ASCE/SEI 7-10 standards, adopted the maximum direction ground motions as the seismic intensity measure to be used in response history analysis of structures (Chapter 21 of ASCE/SEI 7-10).

The maximum direction (MD) orientation angle varies with respect to the given period  $T$ . The assumptions made in using the maximum direction ground motions are (1) the structures properties are identical in all directions (2) azimuth of the maximum spectral acceleration (MD) coincides with principal axis of the the structure.



Basically, structures are either azimuth dependent or azimuth independent. The structural dynamic properties such as stiffness and strength are identical in azimuth independent structures (e.g. bridge piers, silos and chimneys), while they are varying with respect to principal direction of structure in azimuth dependent structures (e.g. dams, bridges). The azimuth independent structures don't have a preferred direction of response, while the azimuth dependent structures have a preferred direction of response. Generally, building structures have different dynamic properties such as stiffness and strength with respect to their main axes (e.g. longitudinal and transverse axes). Somehow, for this reason, structural analysis for lateral load is performed with respect to two main axes buildings. The structural design is often governed by response in the weak axis (transverse direction) of the structure. Even azimuth dependent structures which have identical properties in all directions, have a tendency to the preferred response direction related to their vibration modes. Hence, the first assumption might be valid for structures with a symmetric layout plan. Furthermore, the second assumption is less probable to occur coinciding the maximum direction response with the principal axis of the structures. Stewart et al. (2011), wrote an article undermining use of maximum direction ground motions in the NEHRP seismic maps and likewise, defining maximum direction ground motion for response history analysis of structures in seismic provision of building design codes. The authors argued that it would cause overestimation of design ground motion level by 10 to 30 percent.

## **1.2 SCOPE OF THE RESEARCH**

This study evaluates the effect of building orientation on the structural response of reinforced concrete moment resisting frames with regular and irregular layouts plans. For this purpose, four reinforced concrete moment resisting space frames are modeled in STAAD PRO which consist of symmetric and asymmetric layout plans while each layout is associated with

two natural periods (0.2 second and 1 second period). The natural periods are selected based on ASCE/SEI 7-10 calculation of seismic design loads. Using linear time history analysis in STAAD PRO, all four structures are subjected to a group of 25 ground motion pairs rotated through all non-redundant rotation angles (in this case:  $0^\circ - 180^\circ$ ) with  $5^\circ$  increment using MATLAB software. As the direction of maximum direction ground motions in the near fault regions ( $R_{rup} < 3-5$  km) tend to align with the strike normal direction, in this study all selected ground motions have fault distances greater than 15km to remove the alignment of maximum direction. The plans and 3D models of four computer models are shown in figure 5 through figure 8 with their descriptions in chapter 3 of this thesis.

### **1.3 ORGANIZATION OF THESIS**

This thesis consists of six chapters. The remaining chapters of this thesis is organized as follows:

Chapter 2 is devoted to literature review. It starts with a discussion on record of ground motion acceleration and use of geometric mean of ground motion to produce response spectrum. Next the directionality and need for rotation of ground motions has been discussed, and finally introduction of maximum direction ground motions in the building design codes and its controversy has been discussed accordingly.

Chapter 3 presents the methodology and the details of research carried out in the completion of this thesis. The information for data collection, MATLAB coding for rotation of ground motions, application of rotated ground motions to the structure layouts using STAAD PRO, and generation of results after linear static analysis of the structure layouts in STAAD PRO, have been discussed in detail.

Chapter 4 presents the results of structural response obtained from 25 rotated ground

motion pairs applied to all four types of reinforced concrete moment resisting space frames, after linear static time history analysis by STAAD PRO. It also includes figures showing the structure response of the two proposed layouts for different rotation angles, response corresponding to maximum direction motions. In this chapter, a discussion of results is also included.

Chapter 5 summarizes the results obtained in this thesis and ends with the recommendations for future works to be carried in this study.

## CHAPTER 2

### LITERATURE REVIEW

#### 2.1 GEOMETRIC MEAN OF GROUND MOTIONS:

Generally, the earthquake ground motion accelerations are recorded by accelerometer sensors in three directions (along x,y & z axes), one vertical direction component and two orthogonal horizontal direction components, while the building design codes require only two orthogonal horizontal components of ground motion accelerations for response history analysis of a three-dimensional building structure. The seismic design of structures to withstand lateral loads induced by the earthquake is primarily governed by horizontal ground motion components and the vertical component effects are negligible. The spectral acceleration ( $S_a$ ) cannot be represented in two dimensions. So, there is a need for combining the two orthogonal horizontal components of ground motion or just considering one of the components. Several methods have been proposed in the past to compute spectral acceleration ( $S_a$ ) to represent two-dimensional horizontal ground motions in a single direction. One of the commonly used method, that was acceptable among most of the researchers, is the geometric mean of the two orthogonal horizontal ground motions so-called geometric mean response spectra ( $S_{aGM}$ ). Geometric mean response spectra ( $S_{aGM}$ ), has been traditionally preferred over other methods because it was assumed that it reduces the data dispersion and estimates the central value of arbitrary oriented individual horizontal components of ground motion.

#### 2.2 ROTATION OF GROUND MOTIONS:

On the other hand, using the geometric mean measure of as-recorded ground motions in their arbitrary orientation makes them dependent on the as-recorded orientation of the sensor instrument. Researchers have tried numerous approaches to compute orientation independent

measures of ground motion intensity. Among them, Boore et al. (2006) proposed two forms of orientation independent geometric-mean response spectra for the two recorded orthogonal components. One of them is the period-dependent measure, e.g. GMRotDpp, which D indicates the period-dependency of rotation angle and pp indicates the percentile of the geometric means for sorted amplitudes of all rotation angles. For instance, GMRotD00, GMRotD50 and GMRotD100 are meant to be the maximum, median and minimum geometric mean spectra values respectively over all rotation angles. GMRotDpp is obtained by rotating a pair of ground motion components through all non-redundant rotation angles and selecting a specific percentile from sorted amplitudes of ground motions from all rotations. Another measure proposed by Boore et al. 2006, is GMRotIpp, which was developed to eliminate the unlikable period-dependency of GMRotDpp. Hence, GMRotIpp is defined as the geometric mean measure of the rotated ground motion components to minimize the period inconsistency of GMRotDpp. GMRotIpp is obtained by defining a penalty function of rotation angles to the GMRotDpp measure, computing the angle corresponding to it, and rotating the ground motion pairs through that angle. The authors of Boore et al. (2006) have included a complete algorithmic procedure for calculation of both orientation independent geometric mean measures of ground motion (e.g. GMRotDnn and GMRotInn). The Next Generation Attenuation (NGA) Project employed GMRotI50, for Ground Motion Prediction Equations (GMPEs) which is independent of arbitrary orientation of the recorded ground motion components.

### **2.3 MAXIMUM DIRECTION GROUND MOTIONS:**

The National Earthquake Hazards Reduction Program (NEHRP) Provisions and Commentary 2009 proposed a new measure of ground motions to be used in the seismic design of structures called Maximum Direction (MD) ground motions. Followingly, the US standard

ASCE/SEI 7-10, proposed the maximum direction ground motions to be used in the response history analysis of structures (ASCE/SEI 7-10, Chapter 21). The maximum direction (MD) ground motion is the maximum response of the oscillator regardless of the oscillator's orientation. It can be obtained by finding the maximum response spectra after rotating the ground motion pair through all non-redundant rotation angles or alternatively by plotting the trace of the ground motion pair and finding the furthest point from the origin. Maximum direction (MD) ground motion made it possible for bidirectional ground motions in the horizontal plane to be represented by the maximum spectral pseudo acceleration with a specific period and damping ratio. The maximum direction (MD) ground motion diverges from past practice in earthquake engineering, in which the design spectra were being computed by the geometric mean of the two horizontal components of ground motion. Maximum direction (MD) ground motion intensity measure drew the attention of many researchers to publish several papers on this topic. Campbell and Bozorgnia 2007 & Watson-Lamprey and Boore 2007 observed that the azimuth (orientation) of the maximum direction ground motion is arbitrary for fault distances ( $R_{rup}$ ) larger than approximately 3–5 km, while at closer fault distances, the orientation of the maximum direction (MD) ground motions tends to align with the strike-normal direction. Other researchers tried to develop approximate factors to convert geometric mean ground motion intensity to maximum direction ground motion intensity. Among them, (Bommer et al. 2006, Boore et al. 2007, and Campbell et al. 2007) proposed a maximum direction to geometric mean (MD/GM) ratio of 1.2 to 1.35 depending on period  $T$ . Using different procedures, Huang et al. (2008) found modification factors of maximum direction (MD) ground motion to be 1.1 to 1.5 times the geometric mean ground motions. Moreover, (Boore et al. 2007) noticed that the standard deviation is higher for maximum-direction ground motions than for geometric mean ground

motions. The ground motion hazard maps of the 2009 NEHRP Provisions utilized the factors from Huang et al., 2008, to convert from geometric mean to maximum direction ground motions by factors of 1.1 and 1.3 for short and mid periods respectively. However, (Shahi and Baker 2014) argued that the NEHRP 2009 ratio of 1.1 (short period) was inaccurate and it should be approximately 1.2 (short period).

Use of the new measures of ground motion intensity (maximum direction (MD) ground motion) instead of previously used geometric mean ground motion intensity in NEHRP 2009 provisions found out to be controversial by Stewart et al. (2011). The authors doubted about using maximum direction (MD) ground motion in the NEHRP 2009 and USGS seismic design maps to be unconservative relative to the previously used geometric mean of arbitrary components of ground motions. The authors' doubts were mainly focused on the assumptions made for using the maximum direction (MD) ground motion intensity in the NEHRP 2009 and USGS seismic design maps. Those assumptions are (1) structure's dynamic properties are the same in all directions (2) azimuth of the maximum direction ground motion aligned with the structure's principal axes. The authors argued that these assumptions might be true for some in-plane symmetric structures, but the response of most of the structures is controlled by mode shapes of structures along their specific axes, and usually, they have distinct dynamic properties along those axes. Their research findings show that maximum direction (MD) ground motions applied to structures with azimuth-dependent properties are likely to result in 10% to 30% overestimation of the ground motions depending on the natural period of the structure; this would affect the costs of construction and retrofitting if used in the building codes. In addition to concerns about construction cost, the increase of carbon-related materials in the building's footprint was another concern of authors, while efficiency in the use of materials is necessary for

the sustainability of the environment. Considering all these issues, the authors recommended that for structures with azimuth independent properties, they support the use of the 2009 NEHRP Provisions and following ASCE 7-10 seismic design code, including the existing ground motion design maps. However, for structures with azimuth dependent properties, they recommended use of the 2009 NEHRP Provisions, along with existing site factors and risk factors and following ASCE 7-10 seismic design code except for the ground motion design maps; they suggested use of reduction factors of 1.1 and 1.3 for short and mid periods respectively for using NEHRP seismic design maps until new design maps are prepared by NEHRP.

Following the NEHRP and USGS seismic design maps use of maximum direction (MD) ground motion, the building codes in the United State such as the California Building Code (CBC2010) and also the International Building Code (IBC 2009) with reference to seismic design provisions of ASCE/SEI 7-10, authorized using ground motions rotated to fault normal, fault parallel and maximum direction (MD) ground motions for response history analysis of building structures. According to the mentioned building codes, for time history analysis of a building within 5 kilometers (3.1 miles) from an active fault that dominates the earthquake hazard, the orthogonal ground motion pair should be aligned to the fault normal and fault parallel directions; while for building sites away from the fault source ( $R_{rup} > 5$  km), the maximum direction (MD) ground motions are proposed for response history analysis of buildings. It is believed that the angle corresponding to the FN/FP directions and the maximum direction would lead to the most critical structural response. Subsequently, the United States Geological Survey (USGS) published a research report (Kalkan et al. 2012) on whether to use ground motions rotated to Fault Normal/Parallel or Maximum Direction (MD) direction for response history analysis of buildings, or not. The authors of the USGS report examined the influence of rotation



angle of the ground motion on several engineering demand parameters (EDPs) in linear elastic and nonlinear inelastic domains using a group of computer models of symmetric and asymmetric plan, single-story and multistory buildings subjected to 30 bidirectional near-fault ground motions (i.e. 0.1 km – 15 km), with an average earthquake magnitude of ( $M_w = 6.7 \pm 0.2$ ).

Considering all these criteria, the authors intended to find out whether ground motions rotated to MD or FN/FP directions would lead to the most critical estimates of engineering demand parameters (EDPs) from response history analysis. For this investigation, they have rotated all 30 ground motion pairs from  $0^\circ$  to  $360^\circ$  with a  $5^\circ$  increment and then applied them to all 3D computer models. As mentioned earlier, the previous studies of ground-motion directionality have shown that the azimuth of the maximum direction (MD) ground motion is arbitrary for sites away from the fault ( $R_{rup} > 5$  km) and at near-fault sites ( $R_{rup} < 5$  km) the azimuth of the maximum direction motion tends to align with the strike-normal direction. While findings of the USGS article indicate that the azimuth of the maximum direction motion does not necessarily align with the strike-normal direction even at closer fault distances ( $R_{rup} < 5$  km). Moreover, their study shows that there is no unique orientation for a given structure to maximize all engineering demand parameters (EDPs) simultaneously and the critical angle ( $\theta_{cr}$ ) corresponding to the largest response over all possible rotation angles varies with the ground-motion pair selected, R-value used in the design process and the response quantity EDPs of interest. Finally, the authors of the USGS report conclude that as maximum direction (MD) is not unique for a given ground motion pair and changes with period and R-value of the system, as a result, the maximum direction (MD) response spectrum develops an envelope of the maximum response spectral accelerations of the ground motion pair at all possible rotation angles and periods. Although it was true for linear elastic systems, when they conducted a nonlinear response

history analysis for ground motions oriented in the maximum direction (MD); it did not lead to maximum engineering demand parameters (EDPs) over all orientations in particular for asymmetric plan buildings. Therefore, they claimed that the use of MD ground motion for design is an overly conservative approach. However, the authors still support rotating the bidirectional ground motions at various angles with respect to the structural axes to cover all possible responses for performance assessment and design against worst-case scenarios; and compared to no rotation at all, their research article suggests that the use of ground motions rotated to maximum direction (MD) or fault normal and fault parallel directions is still acceptable.

## CHAPTER 3

### METHODOLOGY AND APPLICATION

#### 3.1 INTRODUCTION:

This chapter describes the process of data collection and using it for analysis. It also describes the computer program that was used in this research. Then it discusses the selection of reinforced concrete frames layouts and their natural periods. Next it describes the algorithm for rotating ground motions and obtaining the maximum direction spectral accelerations.

#### 3.2 GROUND MOTIONS SELECTED (DATA):

For this research, 25 ground motion pairs of records, listed in table 1, were selected from 20 shallow crustal earthquakes compatible with the following configuration:

- Moment magnitude:  $5 \leq M_w \leq 7.62$
- Fault distance:  $R_{rup} \geq 15$  km
- Site classes: A, B, C, D, E

Ground motion data was collected from PEER NGA-West2 ground motion database website(<https://peer.berkeley.edu/peer-strong-ground-motion-databases>). The web-based PEER NGA-West2 ground motion database consist of a very large set of ground motions records from worldwide shallow crustal earthquakes. By creating an account, a user will be able to search, select and download ground motion data from the website. The database gives choice of different distance measure, site characterizations, earthquake source data, etc. Figure 2 shows the distribution of magnitude ( $M_w$ ) versus fault distance ( $R_{rup}$ ) for the 25 ground motion records selected and Figure 3 shows the response spectra of 25 selected ground motion records. As shown in Figure 2, all ground motions were selected for fault distances of more than 15 km ( $R_{rup} > 15$  km) so that the maximum direction orientation would not be affected by fault normal

and fault parallel directions. The maximum direction orientation is assumed to have an arbitrary orientation and will vary with respect to the period of the oscillator. The Figures 4a and 4b show the polar plots of maximum direction spectral accelerations with respect to their rotation angles ( $\theta$ ) for 0.2 second and 1 second natural period of vibration respectively, for 25 ground motions pairs. In these figures, the median spectral acceleration value  $\pm \sigma_n$  (one standard deviation), is shown by red lines. The blue points indicate the maximum direction spectral acceleration with respect to their rotation angle ( $\theta_m$ ) for all 25 ground motion pairs. The blue half-circle lines show the maximum direction median spectral acceleration values  $\pm \sigma_m$  (one standard deviation).

All 25 ground motion pairs were rotated using MATLAB software through all non-redundant rotation angles, in this case from  $0^\circ$  to  $180^\circ$  with a  $5^\circ$  increment. The following formulas from Boore et al. (2006) were used for rotation of ground motion pairs:

$$\ddot{u}_{Rot1} = \ddot{u}_1 \times \cos(\theta) + \ddot{u}_2 \times \sin(\theta) \quad (2)$$

$$\ddot{u}_{Rot2} = -\ddot{u}_1 \times \sin(\theta) + \ddot{u}_2 \times \cos(\theta) \quad (3)$$

where:

$\ddot{u}_{Rot1}$  &  $\ddot{u}_{Rot2}$  = the new rotated acceleration ground motions.

$\ddot{u}_1$  &  $\ddot{u}_2$  = The orthogonal horizontal components of ground motion accelerations.

$\theta$  = Rotation angle, here it takes the values from  $0^\circ$  to  $180^\circ$  with  $5^\circ$  increments.

**Table 1.** Selected ground motion records.

| <i>GM No</i> | <i>Earthquake name</i> | <i>Year</i> | <i>Station Name</i>        | <i>Earthquake magnitude (M<sub>w</sub>)</i> | <i>Fault Mechanism</i> | <i>Fault Distance R<sub>rup</sub>(km)</i> | <i>Site Shear Wave velocity V<sub>s30</sub>(m/s)</i> |
|--------------|------------------------|-------------|----------------------------|---|------------------------|---|--|
| 1            | Humboldt Bay           | 1937        | Ferndale City Hall         | 5.8   | strike slip            | 71.57                                     | 219.31   |
| 2            | Kern County            | 1952        | LA - Hollywood Stor FF     | 7.36  | Reverse                | 117.75                                    | 316.46   |
| 3            | El Alamo               | 1956        | El Centro Array #9         | 6.8   | strike slip            | 121.7                                     | 213.44   |
| 4            | Parkfield              | 1966        | San Luis Obispo            | 6.19  | strike slip            | 63.34                                     | 493.5  |
| 5            | Lytle Creek            | 1970        | Cedar Springs Pump house   | 5.33  | Reverse Oblique        | 22.94                                     | 477.22   |
| 6            | San Fernando           | 1971        | Carbon Canyon Dam          | 6.61  | Reverse                | 61.79                                     | 235  |
| 7            | San Fernando           | 1971        | Lake Hughes #9             | 6.61  | Reverse                | 22.57                                     | 670.84   |
| 8            | San Fernando           | 1971        | Cedar Springs, Allen Ranch | 6.61  | Reverse                | 89.72                                     | 813.48   |
| 9            | Northern Calif-07      | 1975        | Cape Mendocino             | 5.2   | strike slip            | 34.73                                     | 567.78   |
| 10           | Friuli, Italy-01       | 1976        | Codroipo                   | 6.5   | Reverse                | 33.4                                      | 249.28   |
| 11           | Santa Barbara          | 1978        | Cachuma Dam Toe            | 5.92  | Reverse Oblique        | 27.42                                     | 465.51   |
| 12           | Tabas, Iran            | 1978        | Sedeh                      | 7.35  | Reverse                | 151.16                                    | 354.37   |
| 13           | Norcia, Italy          | 1979        | Bevagna                    | 5.9   | Normal                 | 31.45                                     | 401.34   |
| 14           | Loma Prieta            | 1989        | Point Bonita               | 6.93  | Reverse Oblique        | 83.45                                     | 1315.92  |
| 15           | Loma Prieta            | 1989        | Foster City - APEEL 1      | 6.93  | Reverse Oblique        | 43.94                                     | 116.35   |
| 16           | Coalinga-01            | 1983        | Parkfield - Fault Zone 1   | 6.36  | Reverse                | 41.99                                     | 178.27   |
| 17           | Iwate, Japan           | 2008        | IWTH17                     | 6.9   | Reverse                | 72.44                                     | 1269.78  |
| 18           | Chuetsu-oki, Japan     | 2007        | TCGH17                     | 6.8   | Reverse                | 103.85                                    | 1432.75  |
| 19           | Tottori, Japan         | 2000        | OKYH02                     | 6.61  | strike slip            | 70.52                                     | 1047.01  |
| 20           | Chi-Chi, Taiwan-05     | 1999        | HWA003                     | 6.2   | Reverse                | 50.44                                     | 1525.85  |
| 21           | Chi-Chi, Taiwan-06     | 1999        | HWA003                     | 6.3   | Reverse                | 56.02                                     | 1525.85  |
| 22           | Chi-Chi, Taiwan        | 1999        | HWA003                     | 7.62  | Reverse Oblique        | 56.14                                     | 1525.85  |
| 23           | Yountville             | 2000        | APEEL 2 - Redwood City     | 5   | strike slip            | 94.5                                      | 133.11   |
| 24           | Morgan Hill            | 1984        | Foster City - APEEL 1      | 6.19  | strike slip            | 53.89                                     | 116.35   |
| 25           | Niigata                | 2004        | SIT011                     | 6.63  | Reverse                | 173.39                                    | 130.47   |

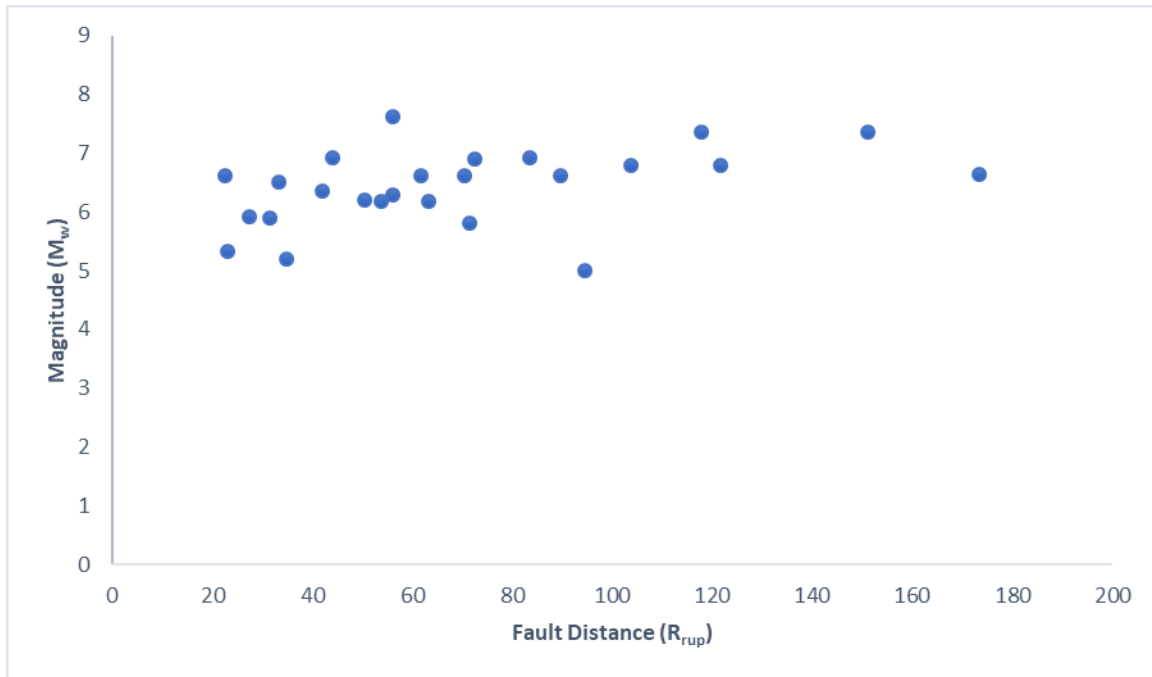


**Figure 2.** Distribution of magnitude ( $M_w$ ) and fault distance ( $R_{rup}$ ) for the 25 ground motion records selected.

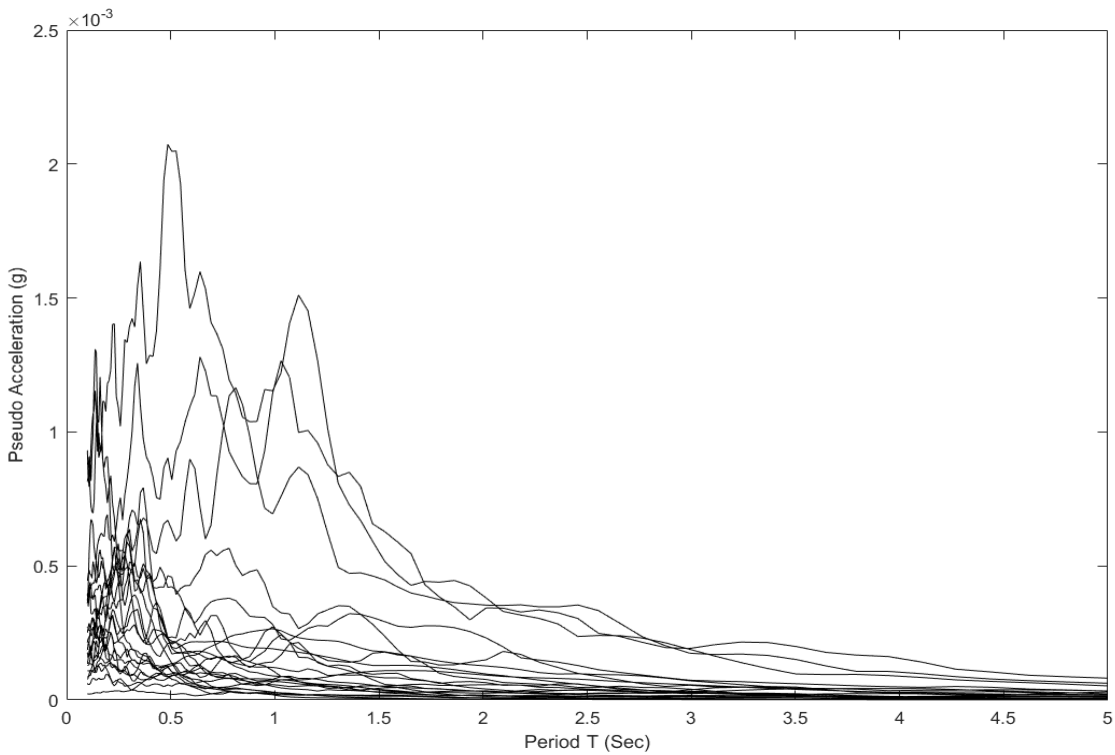
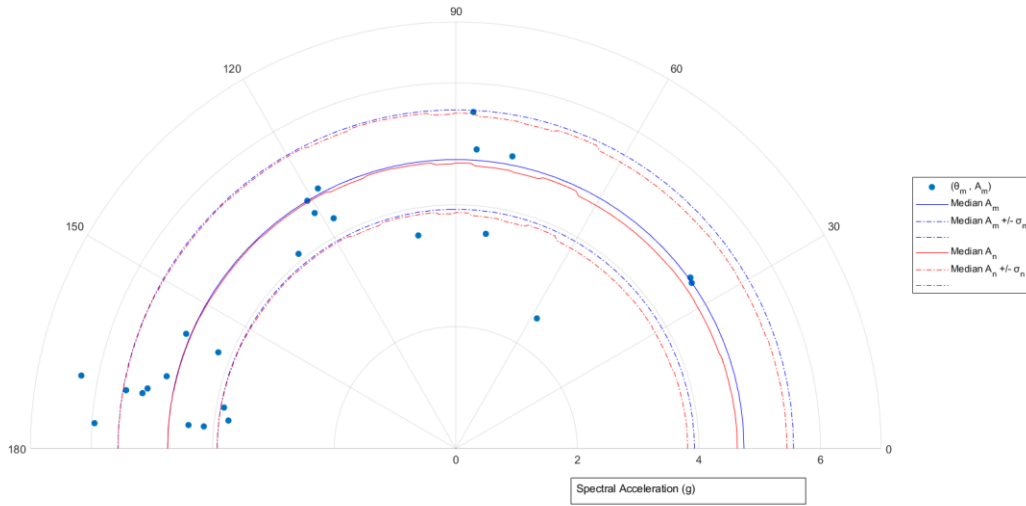
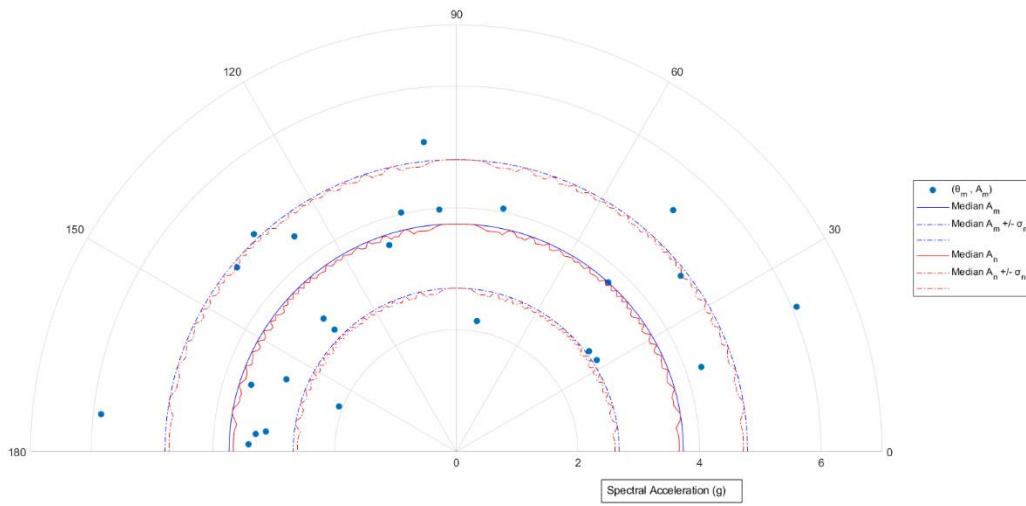


**Figure 3.** Response spectra of 25 ground motion records selected.



(4a)



(4b)

**Figure 4.** Polar plots of spectral acceleration values with respect to rotation angles ( $\theta$ ) for natural vibration periods of 0.2 second (Figure 4a) and 1 second (Figure 4b), for selected 25 ground motion pairs (listed in Table 1). The blue points show the spectral acceleration ( $A_m$ ) with respect to its maximum direction ( $\theta_m$ ) for each ground motion pair. The median spectral accelerations ( $A_n \pm \sigma_n$ ) (one standard deviation) are shown by red lines, and the median spectral acceleration  $\pm \sigma_m$  (one standard deviation) in the maximum direction, is shown by blue half-circle lines.

### **3.3 STAAD PRO:**

STAAD PRO is a structural analysis and design software developed by Bentley Systems Inc. Most of the US and international codes of design for steel and concrete design are included in STAAD PRO. It has the ability to perform all types of linear and non-linear analysis. It has a graphical interface, which makes the structural modeling very easy for the users. In addition, it includes an editor, which enables the user to use command line for structural modeling, analysis and design.

### **3.4 BUILDING MODELS:**

A group of four reinforced concrete moment resisting frame building models were created in STAAD PRO for this research. The building models are:

- 1) A two-story symmetric layout plan building with natural period of 0.2 second (BM1).
- 2) A two-story asymmetric layout plan building with natural period of 0.2 second (BM2).
- 3) A seven-story symmetric layout plan building with natural period of 1 second (BM3).
- 4) A six-story asymmetric layout plan building with natural period of 1 second (BM4).

The plan and 3D view of all four reinforced concrete moment resisting frame building models are shown in Figures 5 through Figure 10. The natural periods of 0.2 second period ( $S_s$ ) and 1 second period ( $S_1$ ) were selected based on the seismic design of buildings in ASCE 7-10. All rectangular shape beam/column cross section area were selected for this research. The concrete of 28-day compressive strength of ( $f_c' = 4000$  psi) and steel reinforcements of grade 60 ( $f_y = 60000$  psi) were provided as construction materials for structural analysis. The dead load, live load, number of stories and column/beam dimensions were selected in such a way to obtain a natural period of 0.2 second and 1 second. The damping ratio of the structure was assumed to



be 5% of critical damping. Fixed support was assumed for all columns.

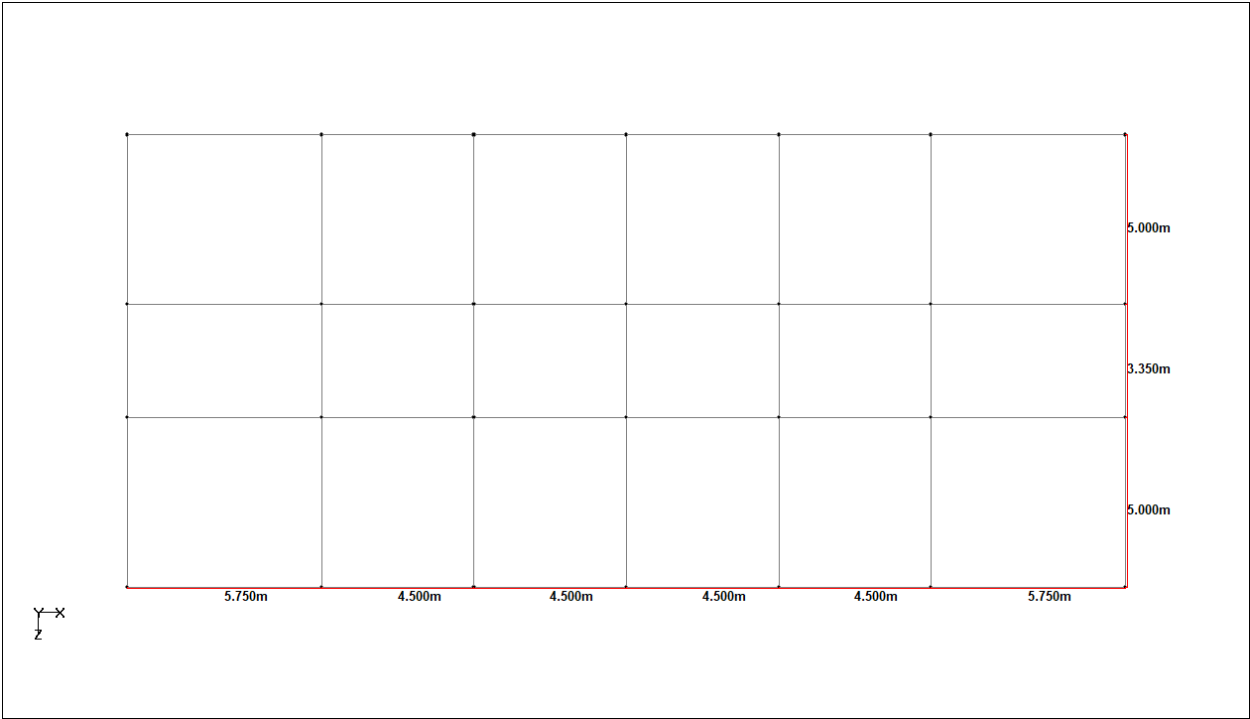


**Figure 5.** Plan view of BM1 and BM3.

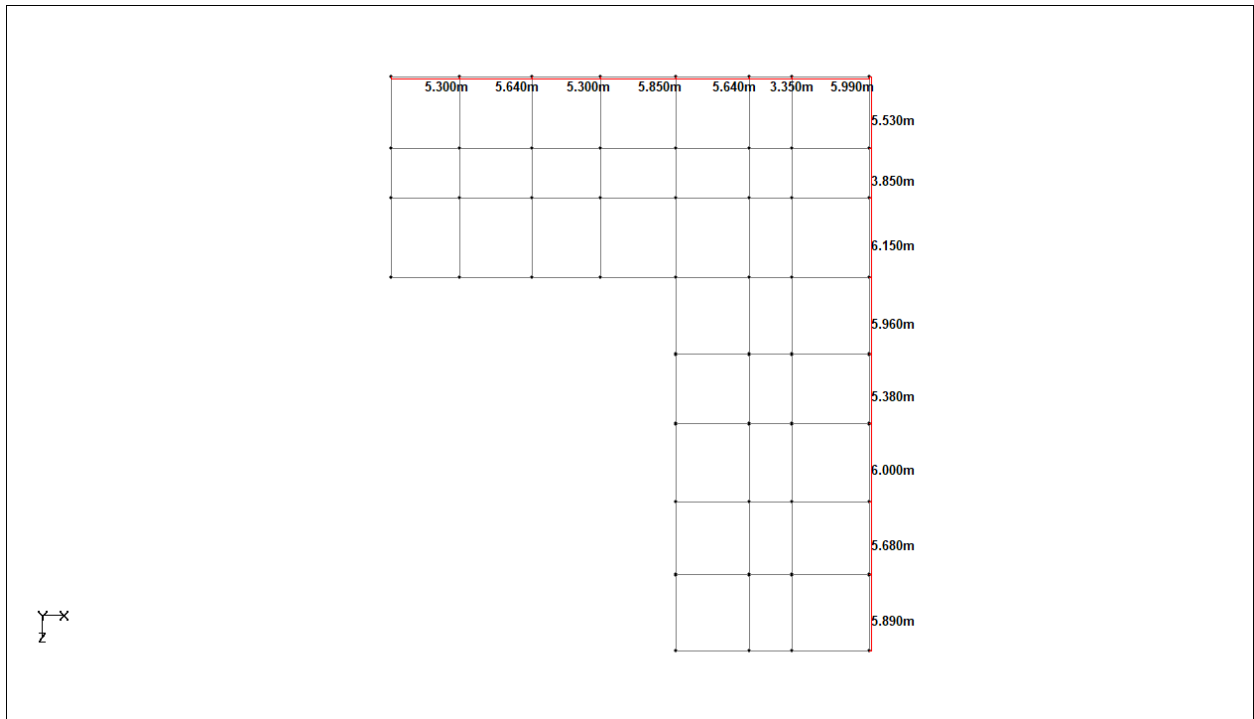


**Figure 6.** Plan view of BM2 and BM4.

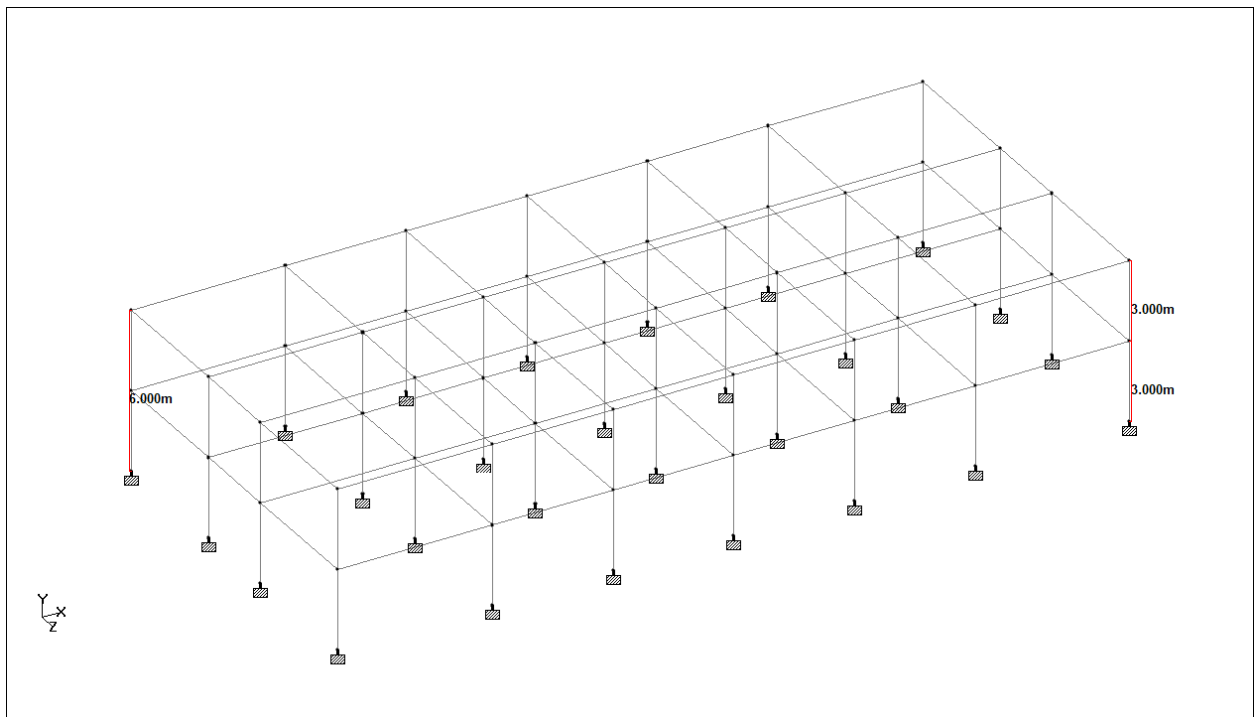


**Figure 7.** 3D view of BM1.

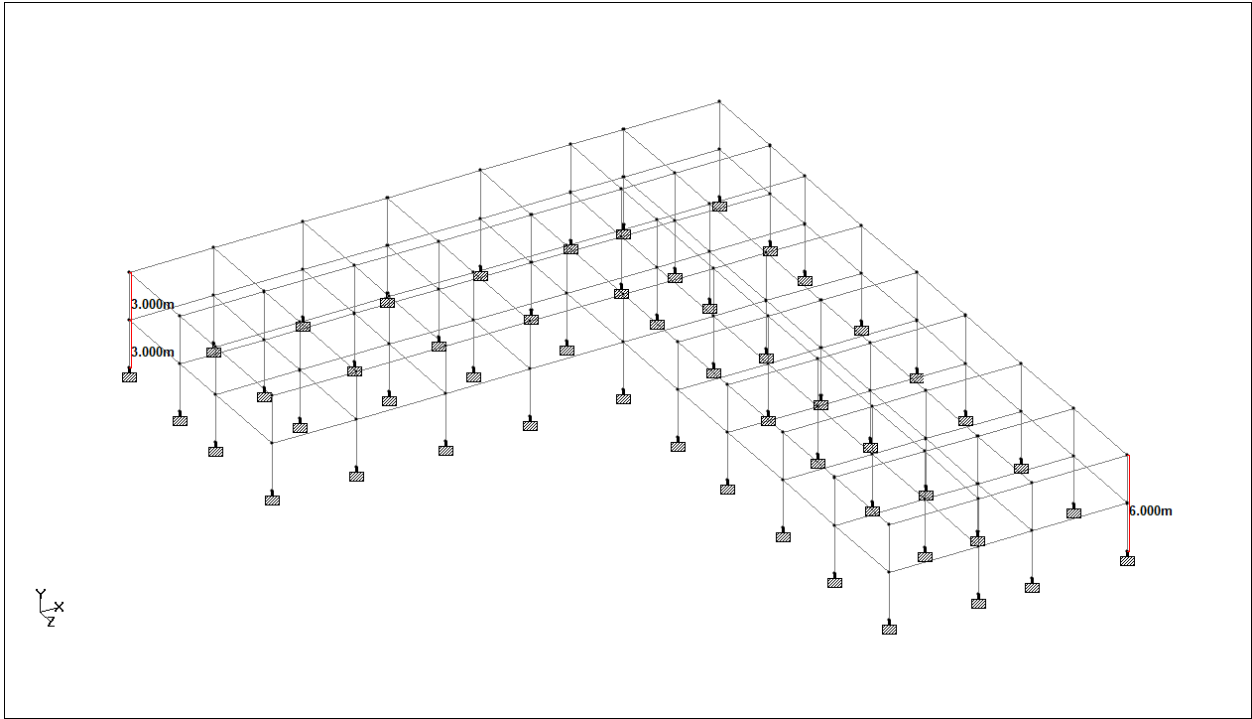


**Figure 8.** 3D view of BM2.

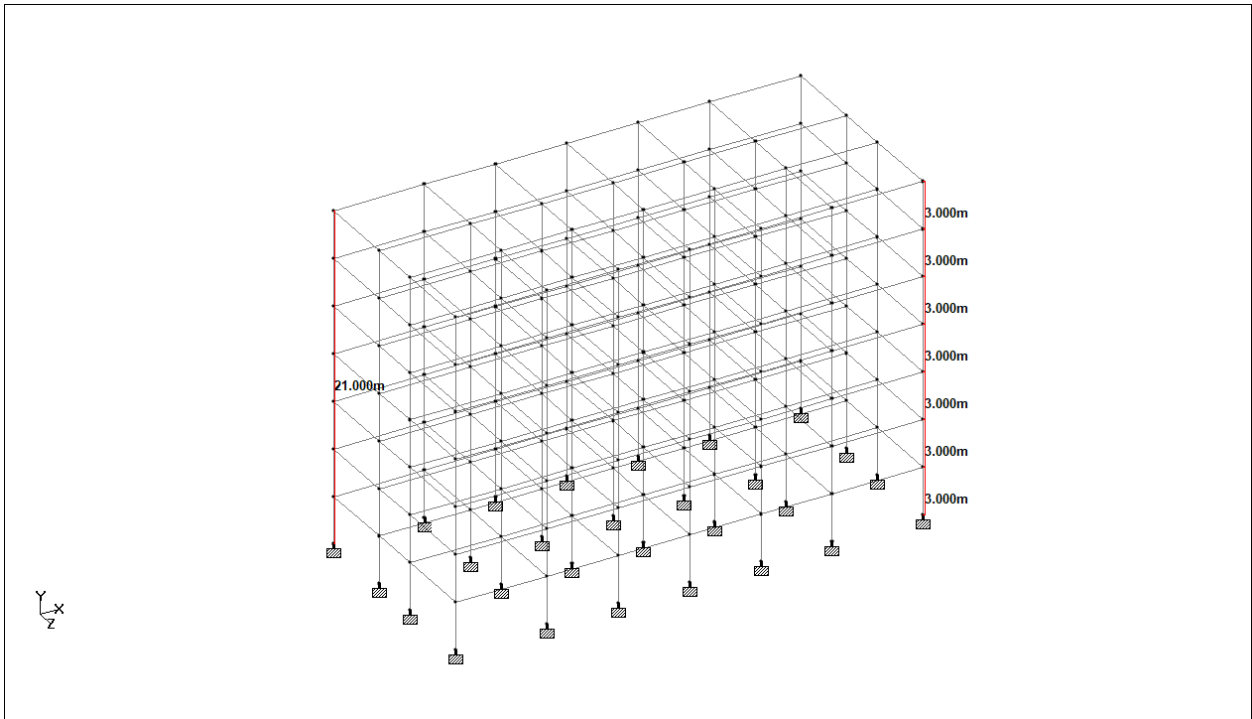


**Figure 9.** 3D view of BM3.

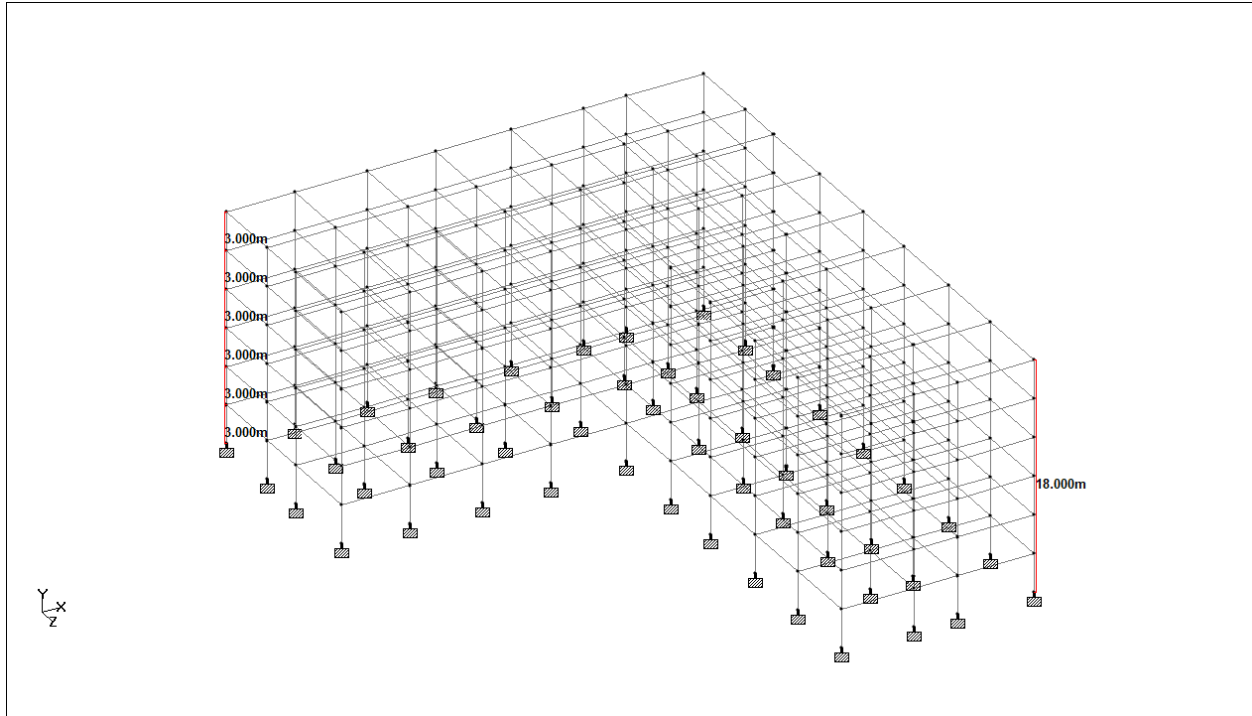


**Figure 10.** 3D view of BM4.

### 3.5 TIME HISTORY ANALYSIS:

Time history analysis is an advanced type of dynamic analysis. It has an ability to incorporate time series accelerations as forcing function. The group of 25 rotated ground motion acceleration pairs (1850 acceleration time series) were used in linear time history analysis in STAAD PRO for each one of 4 building models. The rotated ground motions acceleration time series pairs obtained from Equation 2 & 3 (e.g.  $\ddot{U}_{Rot1}$  &  $\ddot{U}_{Rot2}$ ) were applied to the structures in the form of time series seismic load to “X” and “Z” directions (e.g. longitudinal and transverse directions) of the building models. After the analysis, the structural response (e.g. lateral displacement and story drift) in both directions were recorded for each story of the building models to study effect of building orientation on the structural response. A minimum of 30 mode shapes were defined for the time history analysis to obtain a minimum mass participation factor of 90%.

## CHAPTER 4

### RESULTS AND DISCUSSION

#### 4.1 RESULTS:

The group of 25 ground motion pairs listed in Table 1 were rotated from  $0^\circ$  to  $180^\circ$  with  $5^\circ$  increments, and then using those rotated ground motions pairs, linear time history analysis was performed for four computer building models. The results of time history analysis obtained, are in terms of structure's response (e.g. story drift and lateral displacement) with respect to different building orientations. For this research I have recorded the lateral displacement at center of mass of roof level, and story drifts at center of mass of each floor. These two types of structural responses were recorded for each rotated ground motion pair applied to each computer building model; the total number of structure response cases obtained were 3700. Using the results obtained from time history analysis, separate graphs have been plotted showing the variation of building story drift and lateral displacement at center of mass with respect to building orientation. A complete STAAD PRO analysis and results output for the time history analysis of seven-story rectangular shape (symmetric) building model subjected to GM2 with rotation angle  $30^\circ$ , is included in the Appendix A.

#### 4.2 LATERAL DISPLACEMENT:

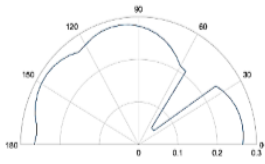
The group of 25 ground motion were rotated from  $0^\circ$  to  $180^\circ$  with  $5^\circ$  increments, then applied to all four building models in terms of time history seismic load in STAAD PRO. After time history analysis, the lateral displacement at center of mass at roof level of all four building models were recorded in X and Z direction of building models, for set of 25 rotated ground motions. Lateral displacement is defined as the displacement of structure in the horizontal direction due to applied horizontal load. The recorded lateral displacement at center of mass was

then plotted with respect to the ground motion rotation angles ( $\theta_x$ ). Figures 11-18 show the variation of lateral displacement at center of mass at roof level with respect to ground motion rotation angle for all four building models subjected to 25 ground motions listed in Table 1.

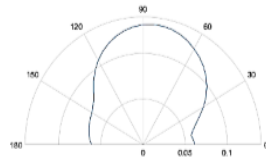
#### **4.3 STORY DRIFT:**

The group of 25 ground motion were rotated from  $0^\circ$  to  $180^\circ$  with  $5^\circ$  increments, then applied to all four building models as seismic load in STAAD PRO. After time history analysis, the story drift at center of mass of each floor for all four building models were recorded in X and Z direction, for each set of rotated ground motions. Here, the story drift is defined as the difference of the lateral displacements at the centers of mass at the top and bottom of the desired story. The recorded story drifts were then plotted with respect to the ground motion rotation angle ( $\theta_x$ ). Figure 19, 20, 22 and 23 show the variation of story drift in the X-direction for each floor level at center of mass with respect to  $\theta_x$  for all four building models subjected to ground motions (GM21, GM16 and GM2). Figure 21 shows the variation of story drift in the X and Z direction for each floor level at center of mass with respect to their rotation angles for rectangular symmetric plan seven-story building model.

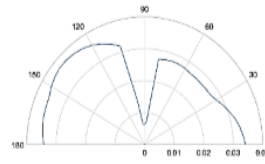




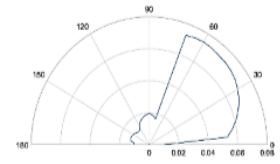
GM16



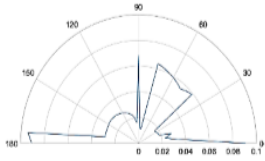
GM17



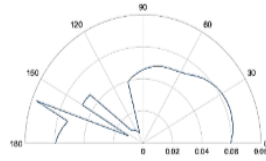
GM18



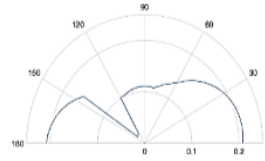
GM19



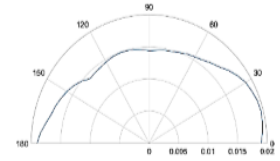
GM20



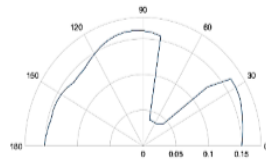
GM21



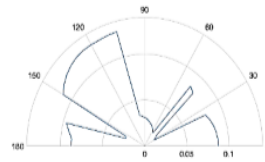
GM22



GM23



GM24

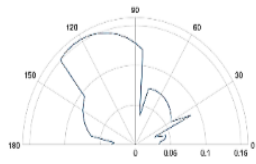


GM25

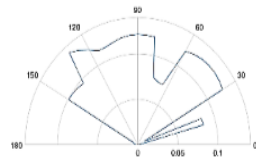
**Figure 11 (b)**

**Figure 11.** Variation of lateral displacement (cm) at roof level ( $U_x$ ) in the X-direction of BM1 at the center of mass (blue line) as a function of the rotation angle,  $\theta_x$ , subjected to 25 ground motions (GM).

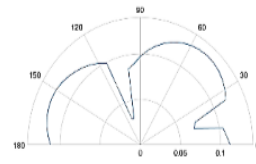




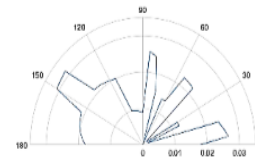
GM1



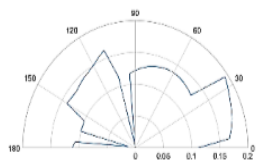
GM2



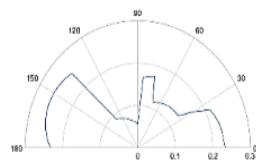
GM3



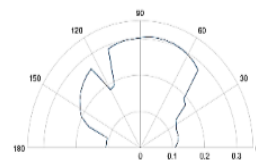
GM4



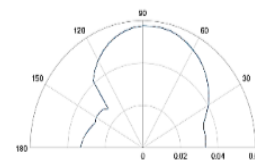
GM5



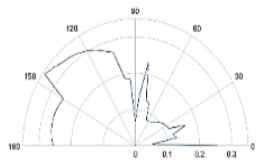
GM6



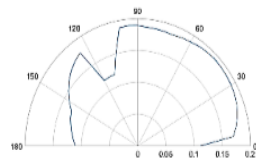
GM7



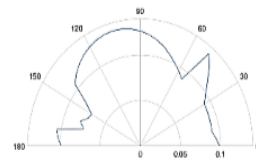
GM8



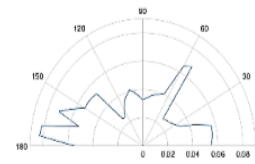
GM9



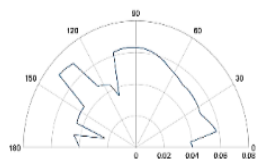
GM10



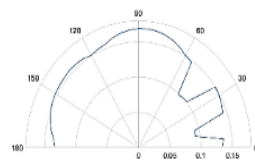
GM11



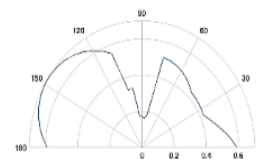
GM12



GM13

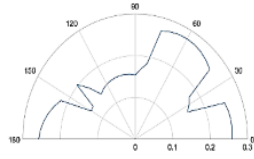


GM14

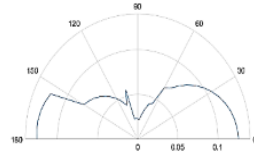


GM15

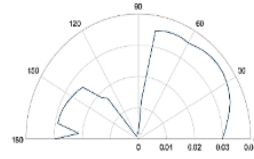
Figure 12 (a)



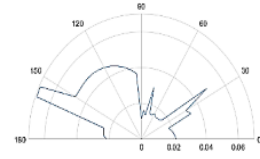
GM16



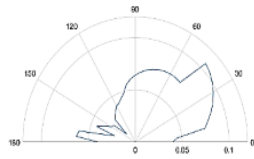
GM17



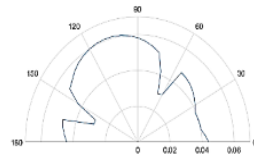
GM18



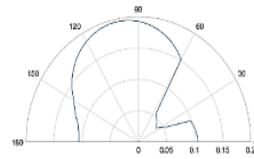
GM19



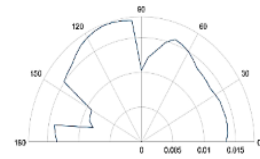
GM20



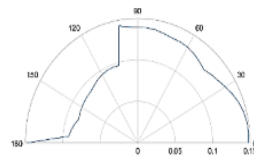
GM21



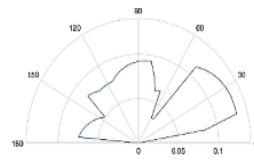
GM22



GM23



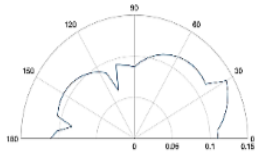
GM24



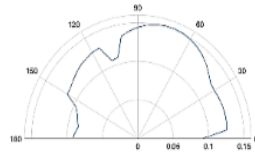
GM25

**Figure 12 (b)**

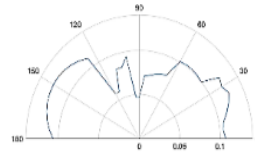
**Figure 12.** Variation of lateral displacement (cm) at roof level ( $U_z$ ) in the Z-direction of BM1 at the center of mass (blue line) as a function of the rotation angle,  $\theta_x$ , subjected to 25 ground motions (GM).



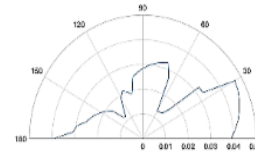
GM1



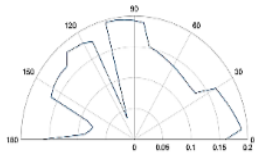
GM2



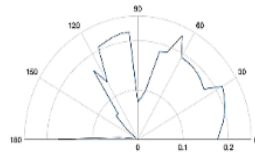
GM3



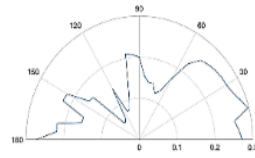
GM4



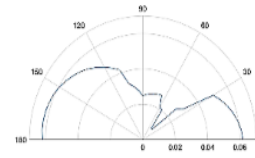
GM5



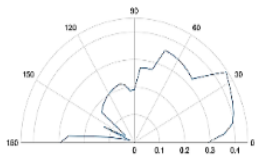
GM6



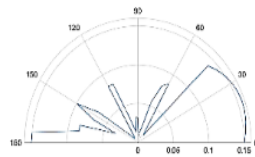
GM7



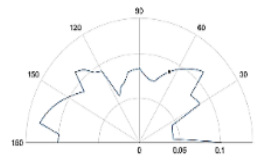
GM8



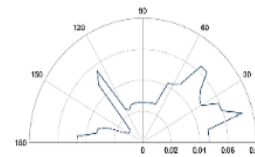
GM9



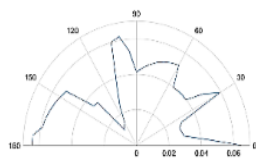
GM10



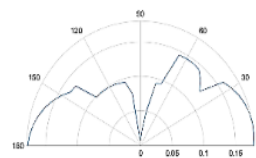
GM11



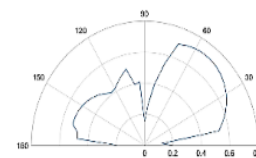
GM12



GM13

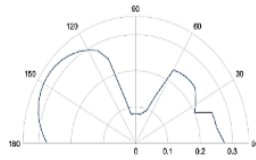


GM14

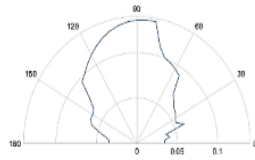


GM15

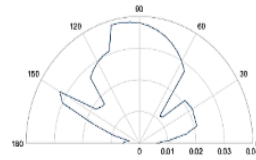
Figure 13 (a)



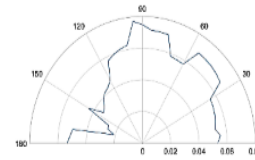
GM16



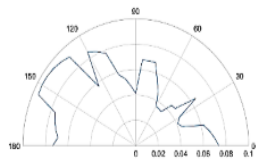
GM17



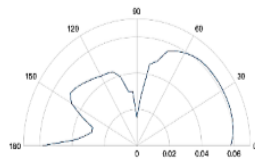
GM18



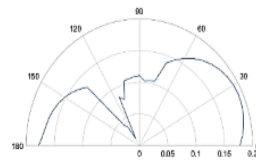
GM19



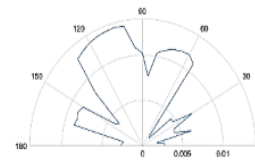
GM20



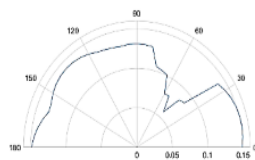
GM21



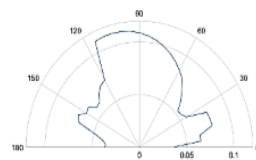
GM22



GM23



GM24



GM25

**Figure 13 (b)**

**Figure 13.** Variation of lateral displacement (cm) at roof level ( $U_x$ ) in the X-direction of BM2 at the center of mass (blue line) as a function of the rotation angle,  $\theta_x$ , subjected to 25 ground motions (GM).



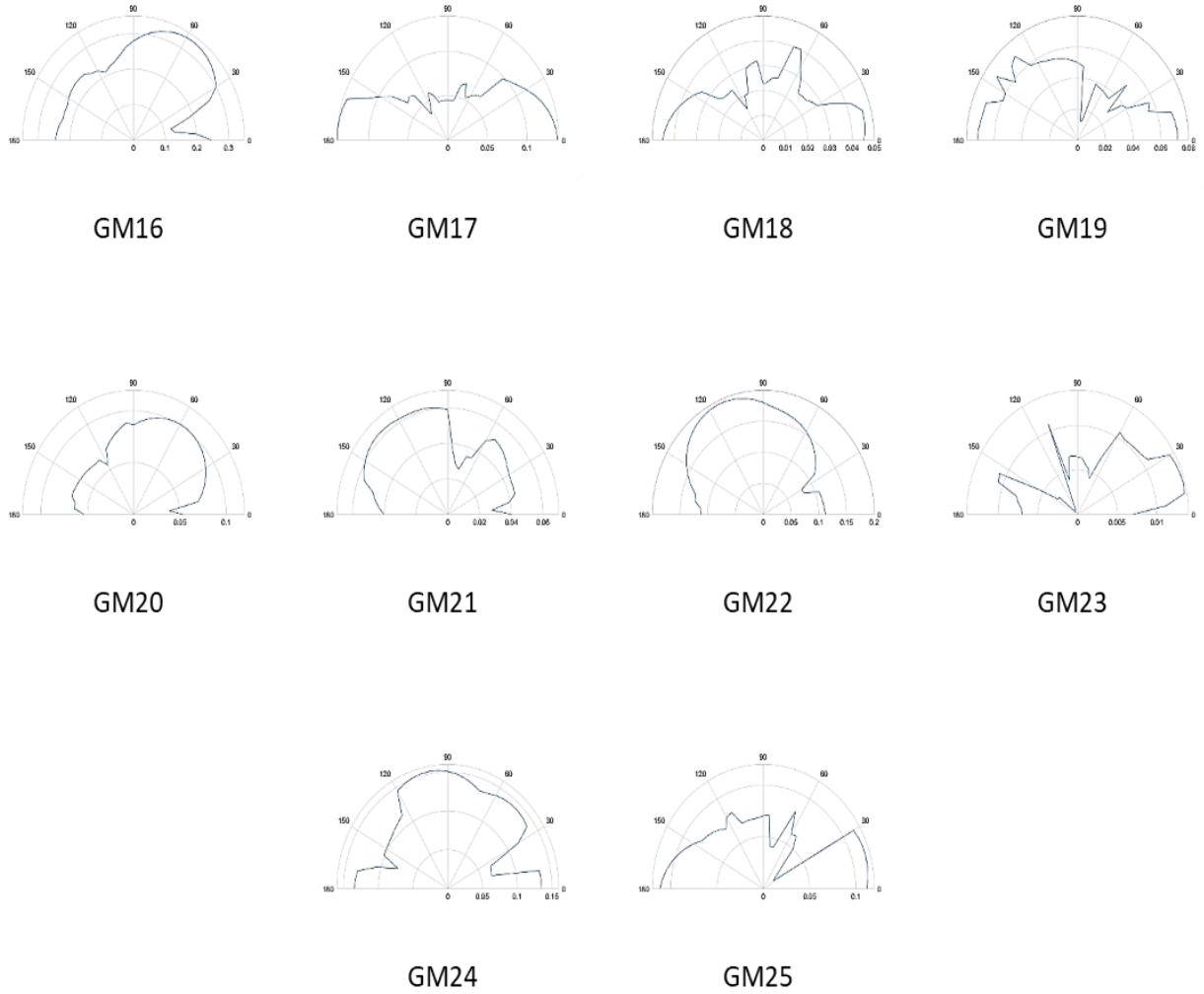
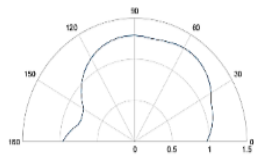
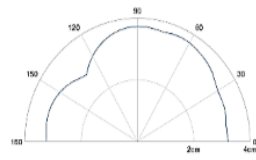


**Figure 14 (b)**

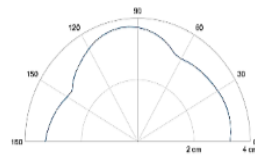
**Figure 14.** Variation of lateral displacement (cm) at roof level ( $U_z$ ) in the Z-direction of BM2 at the center of mass (blue line) as a function of the rotation angle,  $\theta_x$ , subjected to 25 ground motions (GM).



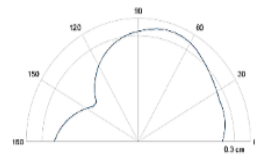
GM1



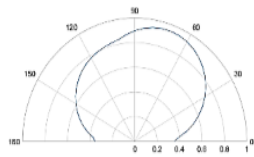
GM2



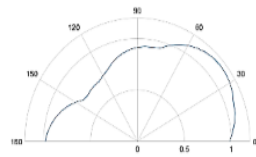
GM3



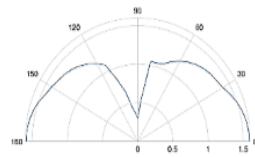
GM4



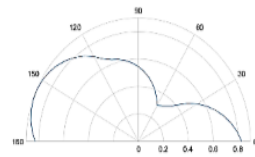
GM5



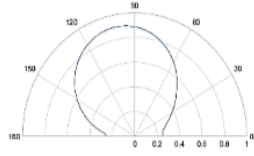
GM6



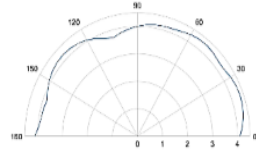
GM7



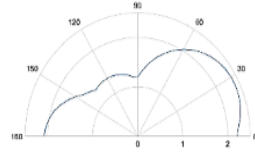
GM8



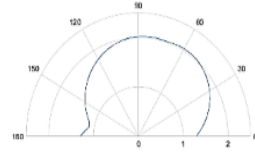
GM9



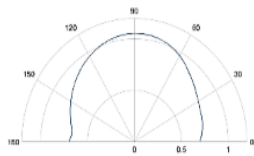
GM10



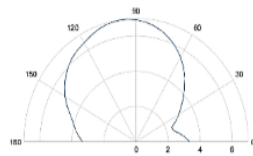
GM11



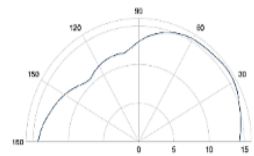
GM12



GM13

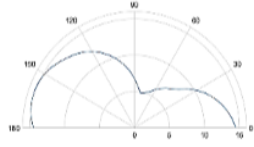


GM14

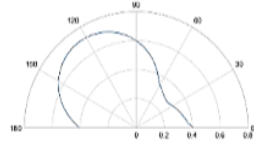


GM15

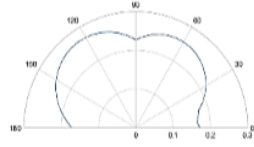
Figure 15 (a)



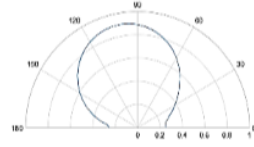
GM16



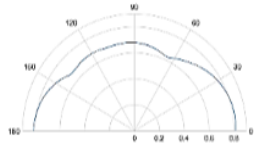
GM17



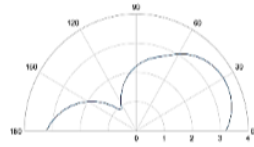
GM18



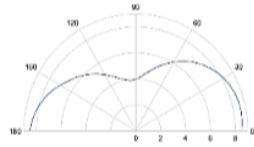
GM19



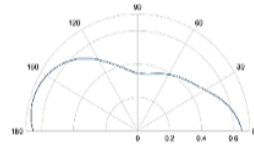
GM20



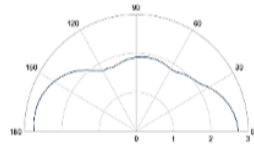
GM21



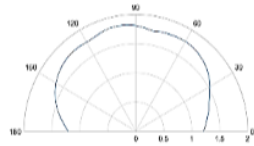
GM22



GM23



GM24

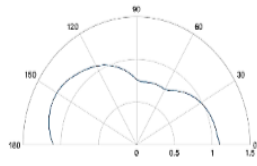


GM25

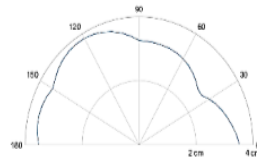
**Figure 15 (b)**

**Figure 15.** Variation of lateral displacement (cm) at roof level ( $U_x$ ) in the X-direction of BM3 at the center of mass (blue line) as a function of the rotation angle,  $\theta_x$ , subjected to 25 ground motions (GM).

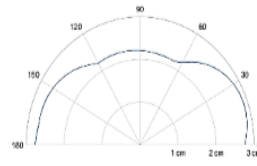




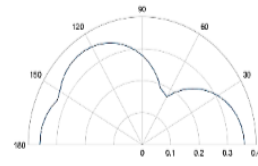
GM1



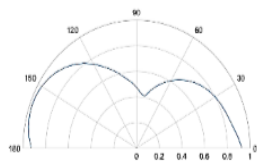
GM2



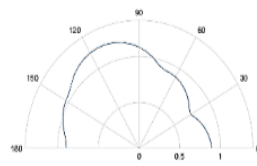
GM3



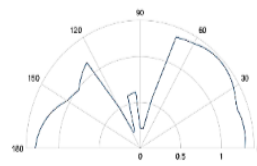
GM4



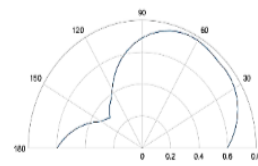
GM5



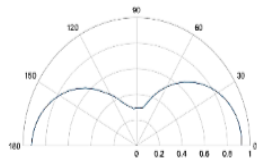
GM6



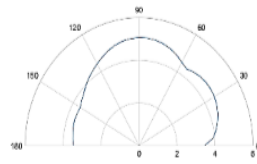
GM7



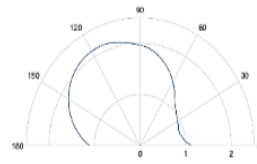
GM8



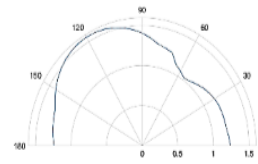
GM9



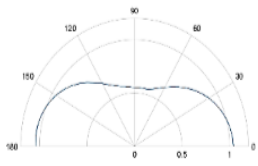
GM10



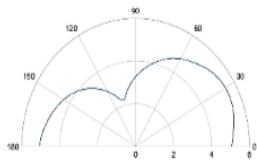
GM11



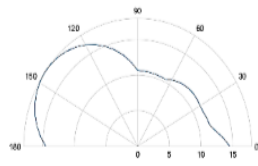
GM12



GM13

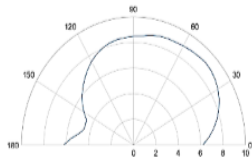


GM14

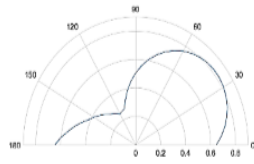


GM15

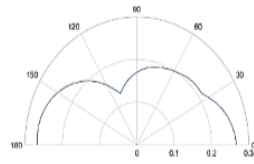
Figure 16 (a)



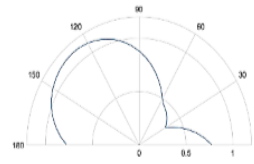
GM16



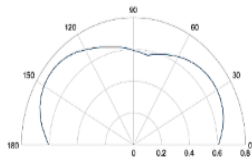
GM17



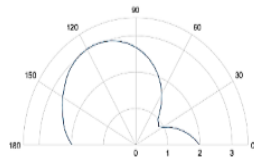
GM18



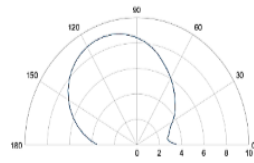
GM19



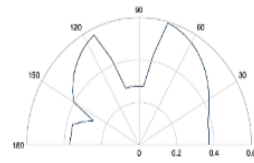
GM20



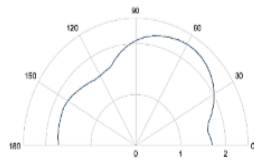
GM21



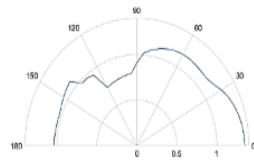
GM22



GM23



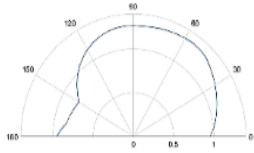
GM24



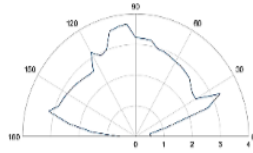
GM25

**Figure 16 (b)**

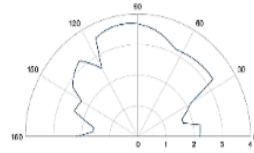
**Figure 16.** Variation of lateral displacement (cm) at roof level ( $U_z$ ) in the Z-direction of BM3 at the center of mass (blue line) as a function of the rotation angle,  $\theta_x$ , subjected to 25 ground motions (GM).



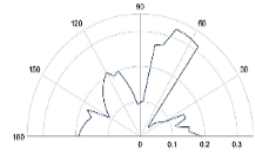
GM1



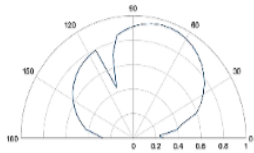
GM2



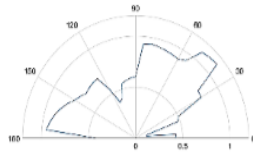
GM3



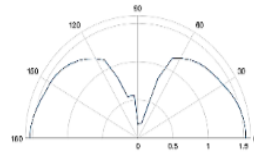
GM4



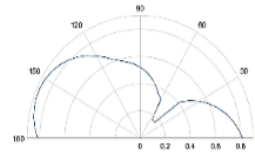
GM5



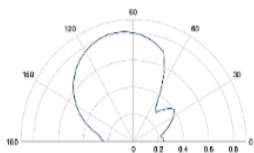
GM6



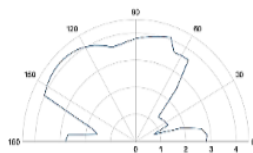
GM7



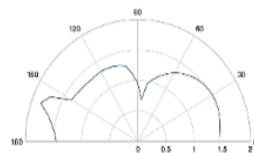
GM8



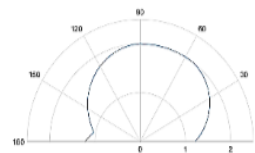
GM9



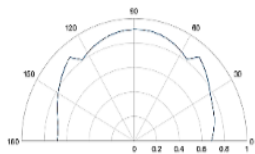
GM10



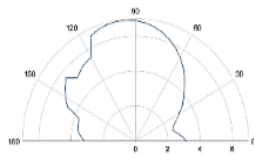
GM11



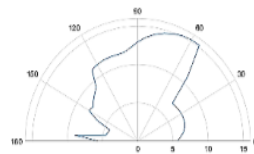
GM12



GM13

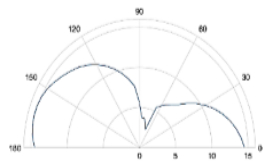


GM14

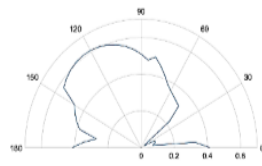


GM15

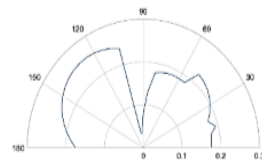
Figure 17 (a)



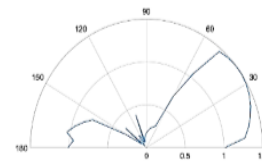
GM16



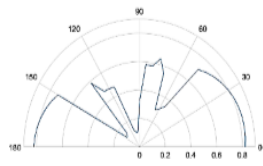
GM17



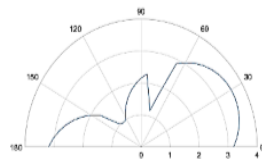
GM18



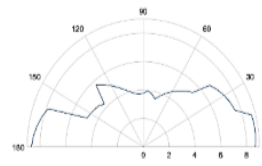
GM19



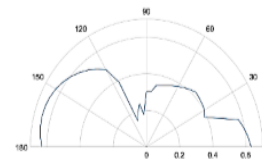
GM20



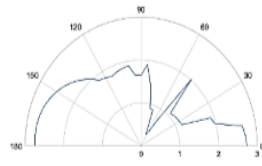
GM21



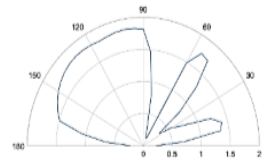
GM22



GM23



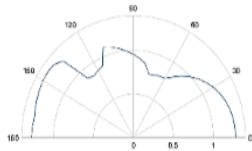
GM24



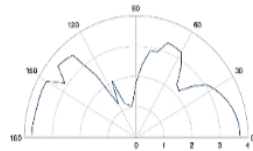
GM25

**Figure 17 (b)**

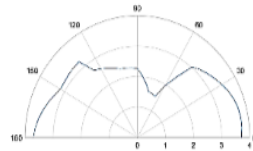
**Figure 17.** Variation of lateral displacement (cm) at roof level ( $U_x$ ) in the X-direction of BM4 at the center of mass (blue line) as a function of the rotation angle,  $\theta_x$ , subjected to 25 ground motions (GM).



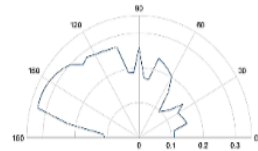
GM1



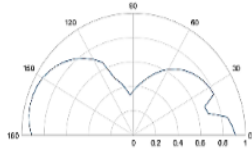
GM2



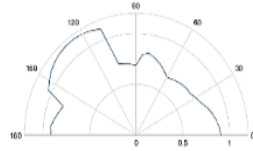
GM3



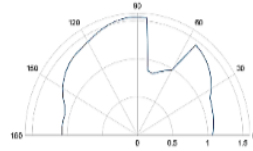
GM4



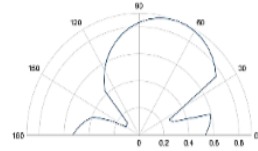
GM5



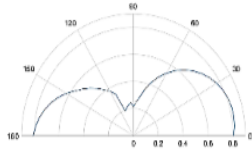
GM6



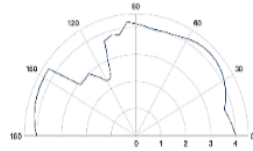
GM7



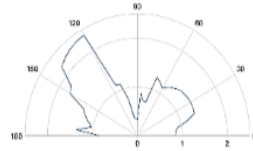
GM8



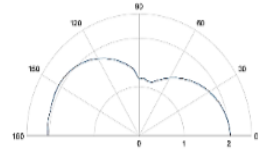
GM9



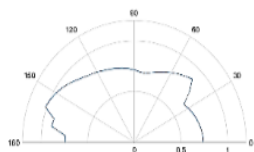
GM10



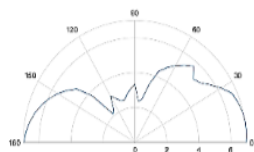
GM11



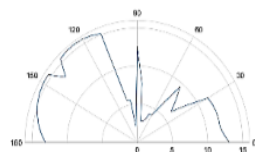
GM12



GM13

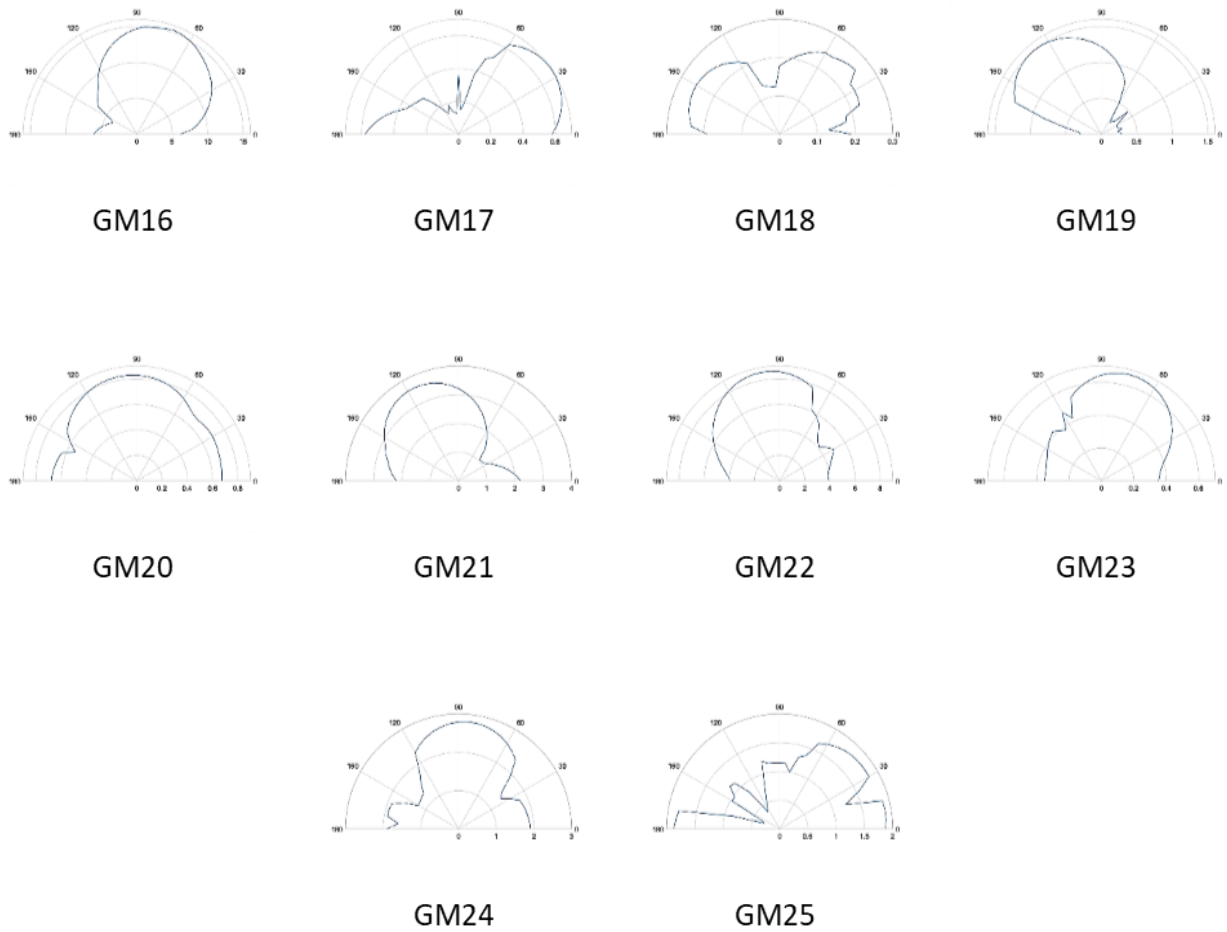


GM14



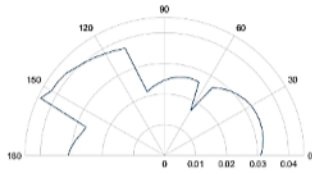
GM15

Figure 18 (a)

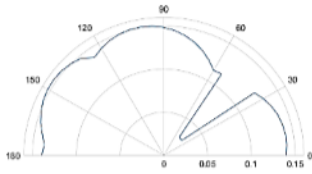


**Figure 18 (b)**

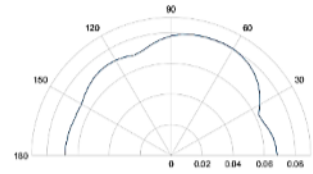
**Figure 18.** Variation of lateral displacement (cm) at roof level ( $U_z$ ) in the Z-direction of BM4 at the center of mass (blue line) as a function of the rotation angle,  $\theta_x$ , subjected to 25 ground motions (GM).



GM21 (1st Floor)

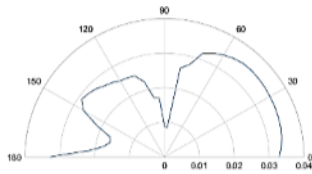


GM16 (1st Floor)

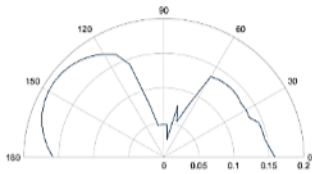


GM2 (1st Floor)

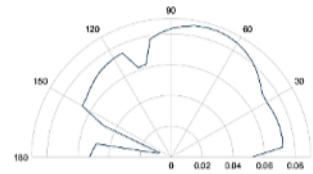
**Figure 19.** Story drifts in the X-direction at center of mass (cm) as a function of rotation angle  $\theta_x$ , for BM1 subjected to ground-motions (GM21, GM16, GM2)



GM21 (1st Floor)



GM16 (1st Floor)



GM2 (1st Floor)

**Figure 20.** Story drifts in the X-direction at center of mass (cm) as a function of rotation angle  $\theta_x$ , for BM2 subjected to ground-motions (GM21, GM16, GM2)

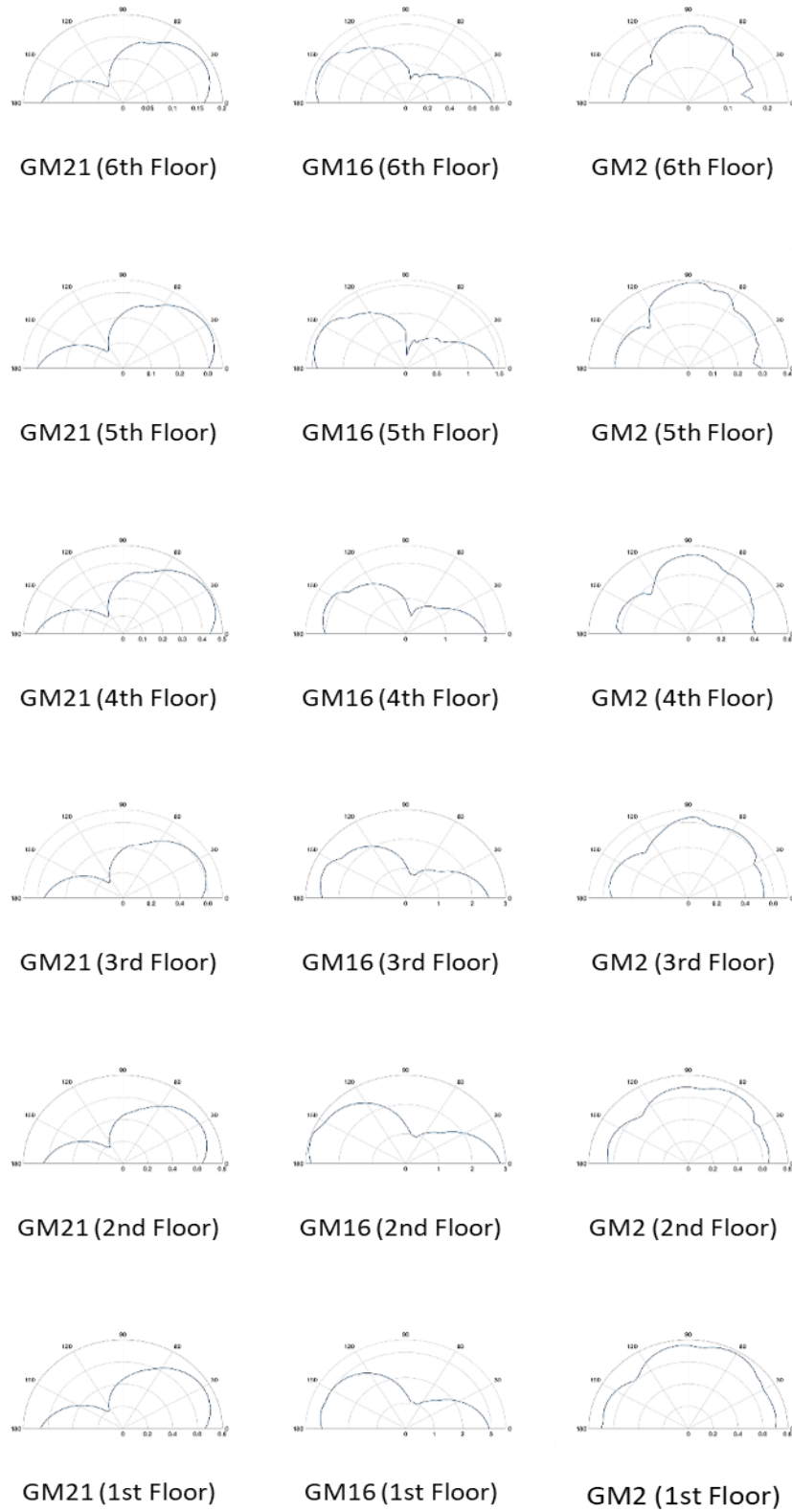


**Figure 21.** Story drifts in the X-direction at center of mass (cm) as a function of rotation angle  $\theta_x$ , for BM3 subjected to ground-motions (GM21, GM16, GM2).



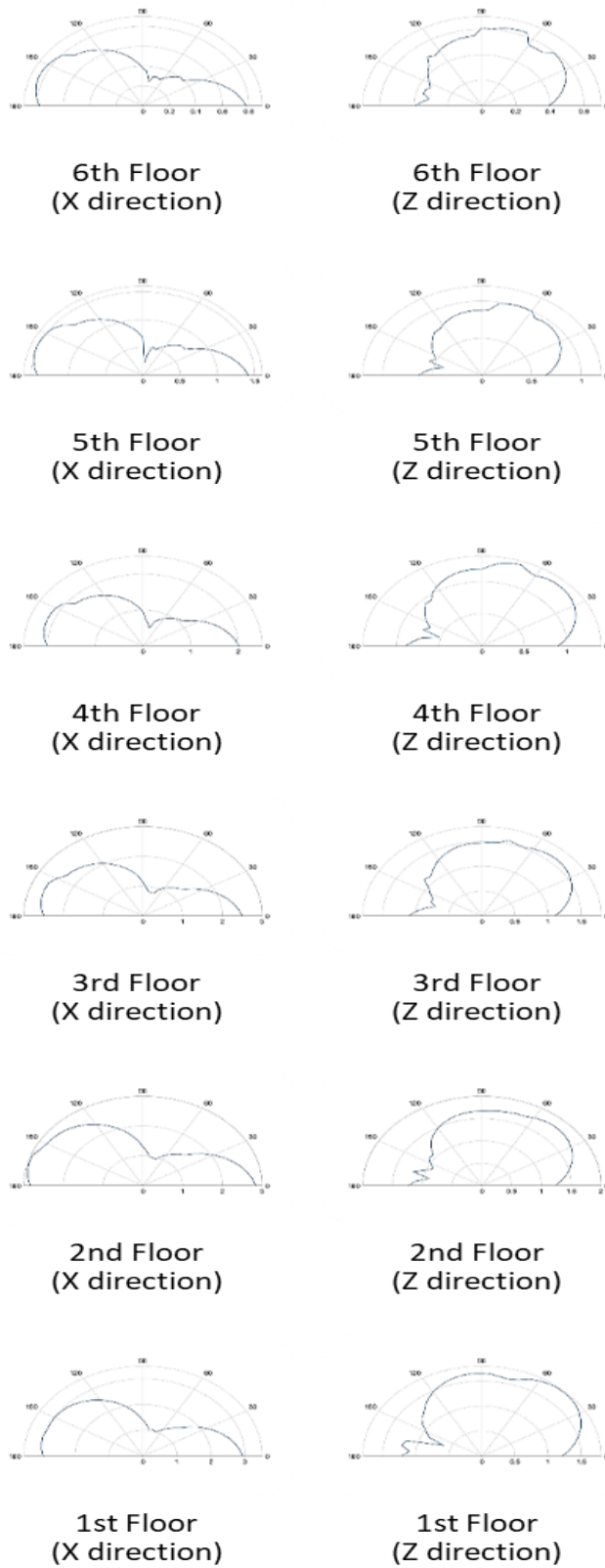


**Figure 22.** Story drifts in the X and Z direction at center of mass (cm) as a function of rotation angle  $\theta_x$ , for BM3 subjected to ground-motion (GM16)

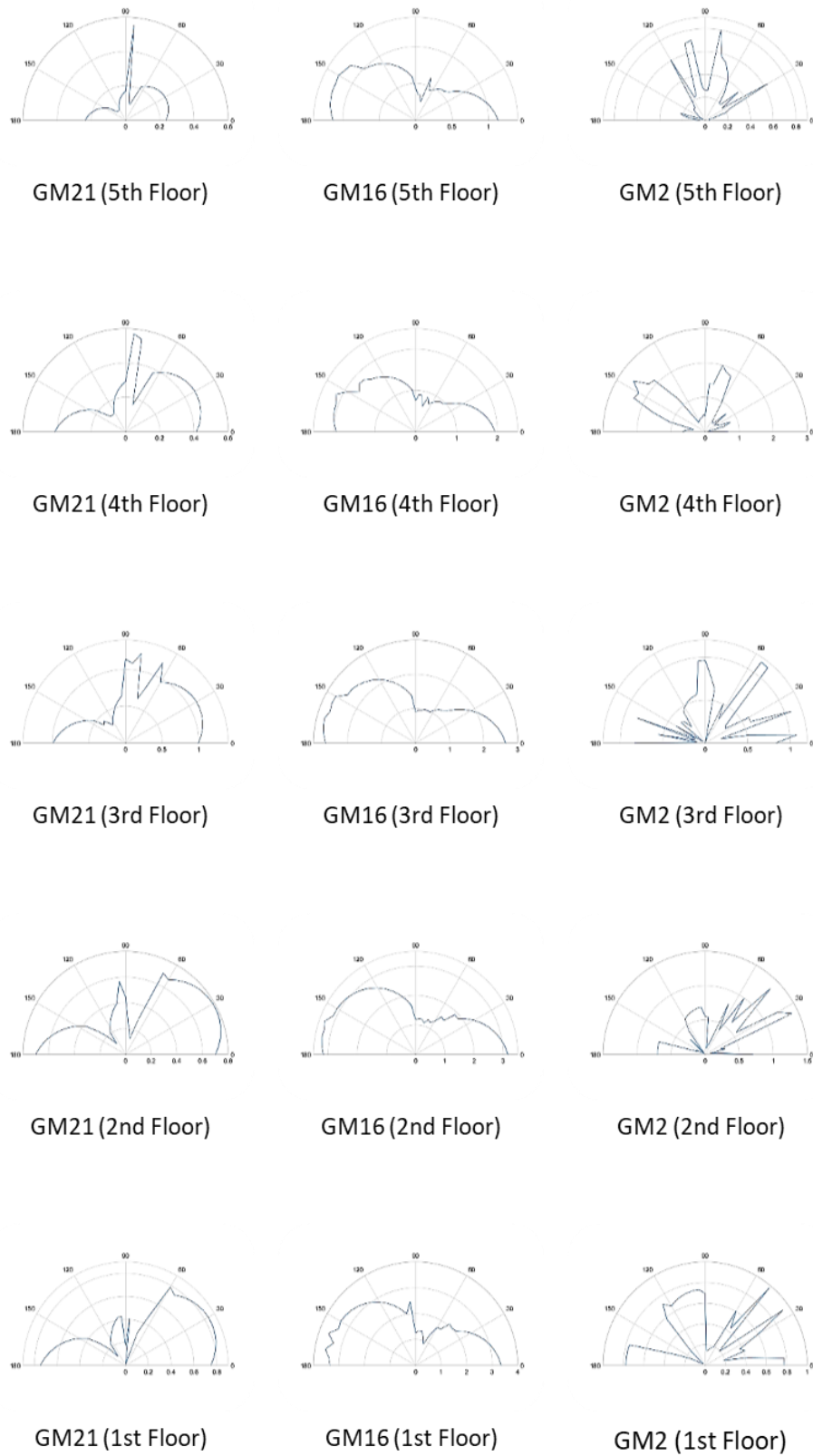


**Figure 23.** Story drifts in the X-direction at center of mass (cm) as a function of rotation angle  $\theta_x$ , for BM4 subjected to ground-motion (GM21, GM16, GM2)

#### 4.4 DISCUSSION:

The results obtained from linear time history analysis of all four reinforced concrete moment resisting frame building models subjected to group of 25 rotated ground motions, shows that the maximum response almost always occurs in an orientation other than the as-recorded orientation of the ground motions. Only in 4.5% of cases (9 out of 200 cases illustrated in figure 11 to 18) the maximum response occurred in as-recorded orientation of the ground motions. This result indicates the significance of the building orientation relative to the direction of application of ground motion in seismic time history analysis of structures. The results obtained from Table 2 in Appendix B (The maximum lateral displacement versus lateral displacement in the as recorded direction of ground motions), the average ratio of maximum response (lateral displacement at roof level) in maximum direction to the response (lateral displacement at roof level) in the as-recorded orientation of ground motions obtained from 25 rotated ground motions applied to 4 reinforced concrete structure building models are as follows:

- 1- Two story symmetric layout plan (BM1) = 3.08
- 2- Two story asymmetric layout plan (BM2) = 2.59
- 3- Seven story symmetric layout plan (BM3) = 1.51
- 4- Six story asymmetric layout plan (BM4) = 1.78

Here, the direction of the maximum structural response is referred to maximum direction, and the as-recorded orientation of the ground motions is referred to the arbitrary orientation.

The plots of lateral displacements at center of mass variation with respect to their rotation angle (figure 11 to 18), indicates that for ground motion with closer fault distances the variation of lateral displacement is polarized to the maximum direction, while for other ground motions away from the fault, there is no sign of polarization. The ratio of maximum response to minimum response is more in the polarized cases than unpolarized cases. This result is true for story drifts

too. These plots indicate that the variation of lateral displacements with respect to their rotation angle, are smooth curves with no rapid changes in structure response in the symmetric layout plan computer models, while for asymmetric layout plan computer models the plots show a discontinuous and broken variation with scattered patterns of rapid change in structure's response of the structure response with respect to their rotation angles.

In time history analysis, the X and Z components of the ground motion were applied to X and Z axes of the building models respectively. The response in the axes of building layout plan (here, X and Z axes), shows different response as the dynamic properties are different along those axes. In this case the vertical loads and stiffness controls the dynamic properties of the structural models, while other properties such as modulus of elasticity, damping ratio and R-value are same for all structural members.

The story drifts at center of mass variation with respect to their rotation angles plots for a given reinforced concrete moment resisting frame model subjected to a ground motion pair rotated through all non-redundant rotation angles indicate that, for symmetric layout plans the story drift plots have almost similar variation in all stories for all non-redundant rotation angles and a unique maximum direction of response, while for asymmetric plans, the story drift plots for different stories show more variation and scattering values and maximum direction of response varies with the floor level. Therefore, the orientation of maximum response not only changes with the natural period of the structure but, it depends on the structure's layout plan.

## CHAPTER 5

### CONCLUSION AND RECOMMENDATIONS

Current seismic design codes of practice in the United States (e.g. ASCE 7-10) requires the ground motion pair to be rotated to Maximum Direction (MD) (The direction which results in the maximum response of the structure) before using them for time history analysis of structures. While it has found out to be controversial by (Stewart et al. 2011). Currently, there has not been enough research conducted to address the effects of ground motion directionality (alternatively building orientation) on nonlinear bidirectional response of structures. In this study, a group of 25 ground motion pairs (listed in table 1) with different fault distances and magnitudes were rotated through all non-redundant rotation angles (e.g.  $0^\circ$  to  $180^\circ$  with  $5^\circ$  increments). Each pair of rotated ground motion were applied through X and Z axes of the computer building models for time history analysis in STAAD PRO. Four computer building models with symmetric and asymmetric plan and first mode of vibration periods of 0.2 second and 1 second were considered for this research. The results obtained from time history analysis of computer building models are in terms of lateral displacement and story drift of structure. The results obtained plotted with respect to their rotation angle using MATLAB. The conclusion of the research carried out in this thesis are as follows:

1. In 95.5% of the analysis cases considered, maximum response occurred in a direction different from the as-recorded directions.
2. The results obtained from symmetric layout plan building models show smooth curves of structural response. The orientation of maximum response in terms of story drift are same for all floors, and orientation of maximum story drift and maximum lateral displacements coincides in all cases.

3. The results obtained from asymmetric layout plan buildings show rapid changes in the structural responses with respect to their rotation angles and the orientation of maximum story drift changes for each floor. In addition, the orientation of maximum story drift and maximum lateral displacement doesn't necessarily coincide.
4. The average ratio of response in the maximum direction to response in the as recorded direction is larger for structures with 0.2 second vibration period than the ones with 1 second period.

### **5.1 RECOMMENDATIONS:**

The recommendations for future studies are as follows:

1. Current research was conducted using linear time history analysis, a non-linear time history analysis needs to be conducted for structures with layout plans and different vibration periods.
2. The effect of building orientation on different types of structural models and materials like steel structures, steel truss, wood structures and concrete shear wall structures needs to be investigated.
3. Seismic behavior of near-fault structures should be investigated separately, as it is known that near-fault records may contain velocity pulses which typically do not coincide with the maximum direction.

## REFERENCES

- American Society of Civil Engineers, 2010, Minimum design loads for buildings and other structures, ASCE/SEI 7-10: Reston, Va., American Society of Civil Engineers, 650 p.
- Beyer, K., and Bommer, J. J., 2006. Relationships between median values and between aleatory variabilities for different definitions of the horizontal component of motion, *Bull Seism Soc Am.* 96, 1512–1522.
- Boore, D. M., Watson-Lamprey, J., and Abrahamson, N. A., 2006. Orientation-independent measures of ground motion, *Bull Seism Soc Am.* 96, 1502–1511.
- Building Seismic Safety Council (BSSC), 2009. NEHRP Recommended Provisions for Seismic Regulations for New Buildings and Other Structures, FEMA P-749, Federal Emergency Management Agency, Washington, D.C.
- Campbell, K.W., and Bozorgnia, Y., 2007, Campbell-Bozorgnia NGA ground motion relations for the geometric mean horizontal component of peak and spectral ground motion parameters: Pacific Earthquake Engineering Research Center, University of California, Berkeley, report no. 2007-02, 238 p.
- Huang, Y., Whittaker, A.S., and Luco, N., 2008, Maximum spectral demands in the near-fault region: *Earthquake Spectra*, v. 24, no.1, p. 319-34.
- International Conference of Building Officials, 2009, International Building Code: Whittier, CA.
- International Conference of Building Officials, 2010, Whittier, Calif., California Building Code.
- Power, Maurice, Brian Chiou, Norman Abrahamson, Yousef Bozorgnia, Thomas Shantz, and Clifford Roblee. "An overview of the NGA project." *Earthquake spectra* 24, no. 1 (2008): 3-21.
- Reyes, Juan C., and Erol Kalkan. Should Ground-motion Records be Rotated to Fault-

- normal/parallel Or Maximum Direction for Response History Analysis of Buildings?. US Department of the Interior, US Geological Survey, 2012.
- Shahi, Shrey K., and Jack W. Baker. "NGA-West2 models for ground motion directionality." *Earthquake Spectra* 30, no. 3 (2014): 1285-1300.
- Stewart, J.P., Abrahamson, N.A., Atkinson, G.M., Baker, J., Boore, D.M., Bozorgnia, Y., Campbell, K.W., Comartin, C.D., Idriss, I.M., Lew, M., Mehrain, M., Moehle, J.P., Naeim, F., and Sabol, T.A., 2011, Representation of bidirectional ground motions for design spectra in building codes: *Earthquake Spectra*, v. 27, no. 3, p. 927–937.
- Watson-Lamprey, J., and Boore, D.M., 2007, Beyond  $S_{aGMRotI}$  Conversion to  $S_{aArb}$ ,  $S_{aSN}$ , and  $S_{aMaxRot}$ : *Bulletin of the Seismological Society of America*, v. 97, p. 1511–1524.



## **APPENDIX A**

### **TIME HISTORY ANALYSIS RESULT**

A complete STAAD PRO analysis and results output for the time history analysis of seven-story rectangular shape (symmetric) building model subjected to GM2 with rotation angle 30°, is included here.

```
*****  
*  
*          STAAD.Pro CONNECT Edition          *  
*          Version 22.02.00.26                *  
*          Proprietary Program of            *  
*          Bentley Systems, Inc.             *  
*          Date=   APR  2, 2020              *  
*          Time=   19:12:50                  *  
*  
*  Licensed to: Student Design Competition site  *  
*****
```

```
1. STAAD SPACE  
INPUT FILE: D:\Thesis\EQ data\data for thesis\GMS(Thesis)\RSN12_KERN.PEL_PEL\Rect(S1).STD  
2. START JOB INFORMATION  
3. ENGINEER DATE 03-SEP-19  
4. END JOB INFORMATION  
5. INPUT WIDTH 79  
6. UNIT METER KN  
7. JOINT COORDINATES  
8. 1 0 0 0; 2 5.75 0 0; 3 10.25 0 0; 4 14.75 0 0; 5 19.25 0 0; 6 23.75 0 0  
9. 7 29.5 0 0; 8 0 3 0; 9 5.75 3 0; 10 10.25 3 0; 11 14.75 3 0; 12 19.25 3 0  
10. 13 23.75 3 0; 14 29.5 3 0; 22 0 0 5; 23 5.75 0 5; 24 10.25 0 5; 25 14.75 0 5  
11. 26 19.25 0 5; 27 23.75 0 5; 28 29.5 0 5; 29 0 3 5; 30 5.75 3 5; 31 10.25 3 5  
12. 32 14.75 3 5; 33 19.25 3 5; 34 23.75 3 5; 35 29.5 3 5; 43 0 0 8.35  
13. 44 5.75 0 8.35; 45 10.25 0 8.35; 46 14.75 0 8.35; 47 19.25 0 8.35  
14. 48 23.75 0 8.35; 49 29.5 0 8.35; 50 0 3 8.35; 51 5.75 3 8.35; 52 10.25 3 8.35  
15. 53 14.75 3 8.35; 54 19.25 3 8.35; 55 23.75 3 8.35; 56 29.5 3 8.35  
16. 64 0 0 13.35; 65 5.75 0 13.35; 66 10.25 0 13.35; 67 14.75 0 13.35  
17. 68 19.25 0 13.35; 69 23.75 0 13.35; 70 29.5 0 13.35; 71 0 3 13.35  
18. 72 5.75 3 13.35; 73 10.25 3 13.35; 74 14.75 3 13.35; 75 19.25 3 13.35  
19. 76 23.75 3 13.35; 77 29.5 3 13.35; 78 0 6 0; 79 5.75 6 0; 80 10.25 6 0  
20. 81 14.75 6 0; 82 19.25 6 0; 83 23.75 6 0; 84 29.5 6 0; 85 0 6 5; 86 5.75 6 5  
21. 87 10.25 6 5; 88 14.75 6 5; 89 19.25 6 5; 90 23.75 6 5; 91 29.5 6 5  
22. 92 0 6 8.35; 93 5.75 6 8.35; 94 10.25 6 8.35; 95 14.75 6 8.35; 96 19.25 6 8.35  
23. 97 23.75 6 8.35; 98 29.5 6 8.35; 99 0 6 13.35; 100 5.75 6 13.35  
24. 101 10.25 6 13.35; 102 14.75 6 13.35; 103 19.25 6 13.35; 104 23.75 6 13.35  
25. 105 29.5 6 13.35; 106 0 9 0; 107 5.75 9 0; 108 10.25 9 0; 109 14.75 9 0  
26. 110 19.25 9 0; 111 23.75 9 0; 112 29.5 9 0; 113 0 9 5; 114 5.75 9 5  
27. 115 10.25 9 5; 116 14.75 9 5; 117 19.25 9 5; 118 23.75 9 5; 119 29.5 9 5  
28. 120 0 9 8.35; 121 5.75 9 8.35; 122 10.25 9 8.35; 123 14.75 9 8.35  
29. 124 19.25 9 8.35; 125 23.75 9 8.35; 126 29.5 9 8.35; 127 0 9 13.35  
30. 128 5.75 9 13.35; 129 10.25 9 13.35; 130 14.75 9 13.35; 131 19.25 9 13.35  
31. 132 23.75 9 13.35; 133 29.5 9 13.35; 134 0 12 0; 135 5.75 12 0; 136 10.25 12 0  
32. 137 14.75 12 0; 138 19.25 12 0; 139 23.75 12 0; 140 29.5 12 0; 141 0 12 5  
33. 142 5.75 12 5; 143 10.25 12 5; 144 14.75 12 5; 145 19.25 12 5; 146 23.75 12 5  
34. 147 29.5 12 5; 148 0 12 8.35; 149 5.75 12 8.35; 150 10.25 12 8.35  
35. 151 14.75 12 8.35; 152 19.25 12 8.35; 153 23.75 12 8.35; 154 29.5 12 8.35  
36. 155 0 12 13.35; 156 5.75 12 13.35; 157 10.25 12 13.35; 158 14.75 12 13.35  
37. 159 19.25 12 13.35; 160 23.75 12 13.35; 161 29.5 12 13.35; 162 0 15 0  
38. 163 5.75 15 0; 164 10.25 15 0; 165 14.75 15 0; 166 19.25 15 0; 167 23.75 15 0
```

STAAD SPACE

-- PAGE NO. 2

39. 168 29.5 15 0; 169 0 15 5; 170 5.75 15 5; 171 10.25 15 5; 172 14.75 15 5  
 40. 173 19.25 15 5; 174 23.75 15 5; 175 29.5 15 5; 176 0 15 8.35; 177 5.75 15 8.35  
 41. 178 10.25 15 8.35; 179 14.75 15 8.35; 180 19.25 15 8.35; 181 23.75 15 8.35  
 42. 182 29.5 15 8.35; 183 0 15 13.35; 184 5.75 15 13.35; 185 10.25 15 13.35  
 43. 186 14.75 15 13.35; 187 19.25 15 13.35; 188 23.75 15 13.35; 189 29.5 15 13.35  
 44. 190 0 18 0; 191 5.75 18 0; 192 10.25 18 0; 193 14.75 18 0; 194 19.25 18 0  
 45. 195 23.75 18 0; 196 29.5 18 0; 197 0 18 5; 198 5.75 18 5; 199 10.25 18 5  
 46. 200 14.75 18 5; 201 19.25 18 5; 202 23.75 18 5; 203 29.5 18 5; 204 0 18 8.35  
 47. 205 5.75 18 8.35; 206 10.25 18 8.35; 207 14.75 18 8.35; 208 19.25 18 8.35  
 48. 209 23.75 18 8.35; 210 29.5 18 8.35; 211 0 18 13.35; 212 5.75 18 13.35  
 49. 213 10.25 18 13.35; 214 14.75 18 13.35; 215 19.25 18 13.35; 216 23.75 18 13.35  
 50. 217 29.5 18 13.35; 218 0 21 0; 219 5.75 21 0; 220 10.25 21 0; 221 14.75 21 0  
 51. 222 19.25 21 0; 223 23.75 21 0; 224 29.5 21 0; 225 0 21 5; 226 5.75 21 5  
 52. 227 10.25 21 5; 228 14.75 21 5; 229 19.25 21 5; 230 23.75 21 5; 231 29.5 21 5  
 53. 232 0 21 8.35; 233 5.75 21 8.35; 234 10.25 21 8.35; 235 14.75 21 8.35  
 54. 236 19.25 21 8.35; 237 23.75 21 8.35; 238 29.5 21 8.35; 239 0 21 13.35  
 55. 240 5.75 21 13.35; 241 10.25 21 13.35; 242 14.75 21 13.35; 243 19.25 21 13.35  
 56. 244 23.75 21 13.35; 245 29.5 21 13.35  
 57. MEMBER INCIDENCES  
 58. 1 8 9; 2 9 10; 3 10 11; 4 11 12; 5 12 13; 6 13 14; 13 1 8; 14 2 9; 15 3 10  
 59. 16 4 11; 17 5 12; 18 6 13; 19 7 14; 27 29 30; 28 30 31; 29 31 32; 30 32 33  
 60. 31 33 34; 32 34 35; 39 22 29; 40 23 30; 41 24 31; 42 25 32; 43 26 33; 44 27 34  
 61. 45 28 35; 53 50 51; 54 51 52; 55 52 53; 56 53 54; 57 54 55; 58 55 56; 65 43 50  
 62. 66 44 51; 67 45 52; 68 46 53; 69 47 54; 70 48 55; 71 49 56; 79 71 72; 80 72 73  
 63. 81 73 74; 82 74 75; 83 75 76; 84 76 77; 91 64 71; 92 65 72; 93 66 73; 94 67 74  
 64. 95 68 75; 96 69 76; 97 70 77; 105 8 29; 106 9 30; 107 10 31; 108 11 32  
 65. 109 12 33; 110 13 34; 111 14 35; 119 29 50; 120 30 51; 121 31 52; 122 32 53  
 66. 123 33 54; 124 34 55; 125 35 56; 133 50 71; 134 51 72; 135 52 73; 136 53 74  
 67. 137 54 75; 138 55 76; 139 56 77; 140 78 79; 141 79 80; 142 80 81; 143 81 82  
 68. 144 82 83; 145 83 84; 146 8 78; 147 9 79; 148 10 80; 149 11 81; 150 12 82  
 69. 151 13 83; 152 14 84; 153 85 86; 154 86 87; 155 87 88; 156 88 89; 157 89 90  
 70. 158 90 91; 159 29 85; 160 30 86; 161 31 87; 162 32 88; 163 33 89; 164 34 90  
 71. 165 35 91; 166 92 93; 167 93 94; 168 94 95; 169 95 96; 170 96 97; 171 97 98  
 72. 172 50 92; 173 51 93; 174 52 94; 175 53 95; 176 54 96; 177 55 97; 178 56 98  
 73. 179 99 100; 180 100 101; 181 101 102; 182 102 103; 183 103 104; 184 104 105  
 74. 185 71 99; 186 72 100; 187 73 101; 188 74 102; 189 75 103; 190 76 104  
 75. 191 77 105; 192 78 85; 193 79 86; 194 80 87; 195 81 88; 196 82 89; 197 83 90  
 76. 198 84 91; 199 85 92; 200 86 93; 201 87 94; 202 88 95; 203 89 96; 204 90 97  
 77. 205 91 98; 206 92 99; 207 93 100; 208 94 101; 209 95 102; 210 96 103  
 78. 211 97 104; 212 98 105; 213 106 107; 214 107 108; 215 108 109; 216 109 110  
 79. 217 110 111; 218 111 112; 219 78 106; 220 79 107; 221 80 108; 222 81 109  
 80. 223 82 110; 224 83 111; 225 84 112; 226 113 114; 227 114 115; 228 115 116  
 81. 229 116 117; 230 117 118; 231 118 119; 232 85 113; 233 86 114; 234 87 115  
 82. 235 88 116; 236 89 117; 237 90 118; 238 91 119; 239 120 121; 240 121 122  
 83. 241 122 123; 242 123 124; 243 124 125; 244 125 126; 245 92 120; 246 93 121  
 84. 247 94 122; 248 95 123; 249 96 124; 250 97 125; 251 98 126; 252 127 128  
 85. 253 128 129; 254 129 130; 255 130 131; 256 131 132; 257 132 133; 258 99 127  
 86. 259 100 128; 260 101 129; 261 102 130; 262 103 131; 263 104 132; 264 105 133  
 87. 265 106 113; 266 107 114; 267 108 115; 268 109 116; 269 110 117; 270 111 118  
 88. 271 112 119; 272 113 120; 273 114 121; 274 115 122; 275 116 123; 276 117 124  
 89. 277 118 125; 278 119 126; 279 120 127; 280 121 128; 281 122 129; 282 123 130  
 90. 283 124 131; 284 125 132; 285 126 133; 286 134 135; 287 135 136; 288 136 137  
 91. 289 137 138; 290 138 139; 291 139 140; 292 106 134; 293 107 135; 294 108 136  
 92. 295 109 137; 296 110 138; 297 111 139; 298 112 140; 299 141 142; 300 142 143  
 93. 301 143 144; 302 144 145; 303 145 146; 304 146 147; 305 113 141; 306 114 142  
 94. 307 115 143; 308 116 144; 309 117 145; 310 118 146; 311 119 147; 312 148 149

STAAD SPACE

-- PAGE NO. 3

95. 313 149 150; 314 150 151; 315 151 152; 316 152 153; 317 153 154; 318 120 148  
 96. 319 121 149; 320 122 150; 321 123 151; 322 124 152; 323 125 153; 324 126 154  
 97. 325 155 156; 326 156 157; 327 157 158; 328 158 159; 329 159 160; 330 160 161  
 98. 331 127 155; 332 128 156; 333 129 157; 334 130 158; 335 131 159; 336 132 160  
 99. 337 133 161; 338 134 141; 339 135 142; 340 136 143; 341 137 144; 342 138 145  
 100. 343 139 146; 344 140 147; 345 141 148; 346 142 149; 347 143 150; 348 144 151  
 101. 349 145 152; 350 146 153; 351 147 154; 352 148 155; 353 149 156; 354 150 157  
 102. 355 151 158; 356 152 159; 357 153 160; 358 154 161; 359 162 163; 360 163 164  
 103. 361 164 165; 362 165 166; 363 166 167; 364 167 168; 365 134 162; 366 135 163  
 104. 367 136 164; 368 137 165; 369 138 166; 370 139 167; 371 140 168; 372 169 170  
 105. 373 170 171; 374 171 172; 375 172 173; 376 173 174; 377 174 175; 378 141 169  
 106. 379 142 170; 380 143 171; 381 144 172; 382 145 173; 383 146 174; 384 147 175  
 107. 385 176 177; 386 177 178; 387 178 179; 388 179 180; 389 180 181; 390 181 182  
 108. 391 148 176; 392 149 177; 393 150 178; 394 151 179; 395 152 180; 396 153 181  
 109. 397 154 182; 398 183 184; 399 184 185; 400 185 186; 401 186 187; 402 187 188  
 110. 403 188 189; 404 155 183; 405 156 184; 406 157 185; 407 158 186; 408 159 187  
 111. 409 160 188; 410 161 189; 411 162 169; 412 163 170; 413 164 171; 414 165 172  
 112. 415 166 173; 416 167 174; 417 168 175; 418 169 176; 419 170 177; 420 171 178  
 113. 421 172 179; 422 173 180; 423 174 181; 424 175 182; 425 176 183; 426 177 184  
 114. 427 178 185; 428 179 186; 429 180 187; 430 181 188; 431 182 189; 432 190 191  
 115. 433 191 192; 434 192 193; 435 193 194; 436 194 195; 437 195 196; 438 162 190  
 116. 439 163 191; 440 164 192; 441 165 193; 442 166 194; 443 167 195; 444 168 196  
 117. 445 197 198; 446 198 199; 447 199 200; 448 200 201; 449 201 202; 450 202 203  
 118. 451 169 197; 452 170 198; 453 171 199; 454 172 200; 455 173 201; 456 174 202  
 119. 457 175 203; 458 204 205; 459 205 206; 460 206 207; 461 207 208; 462 208 209  
 120. 463 209 210; 464 176 204; 465 177 205; 466 178 206; 467 179 207; 468 180 208  
 121. 469 181 209; 470 182 210; 471 211 212; 472 212 213; 473 213 214; 474 214 215  
 122. 475 215 216; 476 216 217; 477 183 211; 478 184 212; 479 185 213; 480 186 214  
 123. 481 187 215; 482 188 216; 483 189 217; 484 190 197; 485 191 198; 486 192 199  
 124. 487 193 200; 488 194 201; 489 195 202; 490 196 203; 491 197 204; 492 198 205  
 125. 493 199 206; 494 200 207; 495 201 208; 496 202 209; 497 203 210; 498 204 211  
 126. 499 205 212; 500 206 213; 501 207 214; 502 208 215; 503 209 216; 504 210 217  
 127. 505 218 219; 506 219 220; 507 220 221; 508 221 222; 509 222 223; 510 223 224  
 128. 511 190 218; 512 191 219; 513 192 220; 514 193 221; 515 194 222; 516 195 223  
 129. 517 196 224; 518 225 226; 519 226 227; 520 227 228; 521 228 229; 522 229 230  
 130. 523 230 231; 524 197 225; 525 198 226; 526 199 227; 527 200 228; 528 201 229  
 131. 529 202 230; 530 203 231; 531 232 233; 532 233 234; 533 234 235; 534 235 236  
 132. 535 236 237; 536 237 238; 537 204 232; 538 205 233; 539 206 234; 540 207 235  
 133. 541 208 236; 542 209 237; 543 210 238; 544 239 240; 545 240 241; 546 241 242  
 134. 547 242 243; 548 243 244; 549 244 245; 550 211 239; 551 212 240; 552 213 241  
 135. 553 214 242; 554 215 243; 555 216 244; 556 217 245; 557 218 225; 558 219 226  
 136. 559 220 227; 560 221 228; 561 222 229; 562 223 230; 563 224 231; 564 225 232  
 137. 565 226 233; 566 227 234; 567 228 235; 568 229 236; 569 230 237; 570 231 238  
 138. 571 232 239; 572 233 240; 573 234 241; 574 235 242; 575 236 243; 576 237 244  
 139. 577 238 245  
 140. DEFINE MATERIAL START  
 141. ISOTROPIC CONCRETE  
 142. E 2.17185E+07  
 143. POISSON 0.17  
 144. DENSITY 23.5616  
 145. ALPHA 1E-05  
 146. DAMP 0.05  
 147. TYPE CONCRETE  
 148. STRENGTH FCU 27579  
 149. END DEFINE MATERIAL  
 150. MEMBER PROPERTY AMERICAN

STAAD SPACE

-- PAGE NO. 4

151. 13 TO 19 39 TO 45 65 TO 71 91 TO 97 146 TO 152 159 TO 165 172 TO 178 -  
 152. 185 TO 191 219 TO 225 232 TO 238 245 TO 251 258 TO 264 292 TO 298 -  
 153. 305 TO 311 318 TO 324 331 TO 337 365 TO 371 378 TO 384 391 TO 397 -  
 154. 404 TO 410 438 TO 444 451 TO 457 464 TO 470 477 TO 483 511 TO 517 -  
 155. 524 TO 530 537 TO 543 550 TO 556 PRIS YD 0.5 ZD 0.7  
 156. 1 TO 6 27 TO 32 53 TO 58 79 TO 84 105 TO 111 119 TO 125 133 TO 145 -  
 157. 153 TO 158 166 TO 171 179 TO 184 192 TO 218 226 TO 231 239 TO 244 -  
 158. 252 TO 257 265 TO 291 299 TO 304 312 TO 317 325 TO 330 338 TO 364 -  
 159. 372 TO 377 385 TO 390 398 TO 403 411 TO 437 445 TO 450 458 TO 463 -  
 160. 471 TO 476 484 TO 510 518 TO 523 531 TO 536 544 TO 549 557 TO 576 -  
 161. 577 PRIS YD 0.6 ZD 0.4  
 162. CONSTANTS  
 163. MATERIAL CONCRETE ALL  
 164. SUPPORTS  
 165. 1 TO 7 22 TO 28 43 TO 49 64 TO 70 FIXED  
 166. DEFINE TIME HISTORY  
 167. TYPE 1 ACCELERATION  
 168. READ KERN\_PEL\_X30.TXT  
 169. TYPE 2 ACCELERATION  
 170. READ KERN\_PEL\_Z30.TXT  
 171. ARRIVAL TIME  
 172. 0  
 173. DAMPING 0.05  
 174. CUT OFF MODE SHAPE 30  
 175. LOAD 1 LOADTYPE DEAD TITLE DL  
 176. SELFWEIGHT Y -1  
 177. MEMBER LOAD  
 178. 27 TO 32 53 TO 58 106 TO 110 134 TO 138 153 TO 158 166 TO 171 193 TO 197 207 -  
 179. 208 TO 211 226 TO 231 239 TO 244 266 TO 270 280 TO 284 299 TO 304 312 TO 317 -  
 180. 339 TO 343 353 TO 357 372 TO 377 385 TO 390 412 TO 416 426 TO 430 -  
 181. 445 TO 450 458 TO 463 485 TO 489 499 TO 503 518 TO 523 531 TO 536 -  
 182. 558 TO 562 572 TO 576 UNI GY -4.9  
 183. 1 TO 6 68 71 79 TO 84 105 111 119 125 133 139 TO 145 175 178 TO 184 192 198 -  
 184. 199 205 206 212 TO 218 248 251 TO 257 265 271 272 278 279 285 TO 291 321 -  
 185. 324 TO 330 338 344 345 351 352 358 TO 364 394 397 TO 403 411 417 418 424 -  
 186. 425 431 TO 437 467 470 TO 476 484 490 491 497 498 504 TO 510 540 543 TO 549 -  
 187. 557 563 564 570 571 577 UNI GY -15.12  
 188. FLOOR LOAD  
 189. YRANGE 0 21 FLOAD -5.8 XRANGE 0 29.5 ZRANGE 0 13.35 GY  
**\*\*NOTE\*\* about Floor/OneWay Loads/Weights.**  
 Please note that depending on the shape of the floor you may  
 have to break up the FLOOR/ONEWAY LOAD into multiple commands.  
 For details please refer to Technical Reference Manual  
 Section 5.32.4.2 Note d and/or "5.32.4.3 Note f."  
 190. LOAD 2 LOADTYPE LIVE TITLE LL  
 191. FLOOR LOAD  
 192. YRANGE 0 21 FLOAD -4 XRANGE 0 29.5 ZRANGE 0 13.35 GY  
 193. LOAD 3 LOADTYPE SEISMIC TITLE DYNAMIC LOAD  
 194. SELFWEIGHT X 1

STAAD SPACE

-- PAGE NO. 5

195. SELFWEIGHT Y 1  
 196. SELFWEIGHT Z 1  
 197. MEMBER LOAD  
 198. 27 TO 32 53 TO 58 106 TO 110 134 TO 138 153 TO 158 166 TO 171 193 TO 197 207 -  
 199. 208 TO 211 226 TO 231 239 TO 244 266 TO 270 280 TO 284 299 TO 304 312 TO 317 -  
 200. 339 TO 343 353 TO 357 372 TO 377 385 TO 390 412 TO 416 426 TO 430 -  
 201. 445 TO 450 458 TO 463 485 TO 489 499 TO 503 518 TO 523 531 TO 536 -  
 202. 558 TO 562 572 TO 576 UNI GX 4.9  
 203. 27 TO 32 53 TO 58 106 TO 110 134 TO 138 153 TO 158 166 TO 171 193 TO 197 207 -  
 204. 208 TO 211 226 TO 231 239 TO 244 266 TO 270 280 TO 284 299 TO 304 312 TO 317 -  
 205. 339 TO 343 353 TO 357 372 TO 377 385 TO 390 412 TO 416 426 TO 430 -  
 206. 445 TO 450 458 TO 463 485 TO 489 499 TO 503 518 TO 523 531 TO 536 -  
 207. 558 TO 562 572 TO 576 UNI GY 4.9  
 208. 27 TO 32 53 TO 58 106 TO 110 134 TO 138 153 TO 158 166 TO 171 193 TO 197 207 -  
 209. 208 TO 211 226 TO 231 239 TO 244 266 TO 270 280 TO 284 299 TO 304 312 TO 317 -  
 210. 339 TO 343 353 TO 357 372 TO 377 385 TO 390 412 TO 416 426 TO 430 -  
 211. 445 TO 450 458 TO 463 485 TO 489 499 TO 503 518 TO 523 531 TO 536 -  
 212. 558 TO 562 572 TO 576 UNI GZ 4.9  
 213. 1 TO 6 68 71 79 TO 84 105 111 119 125 133 139 TO 145 175 178 TO 184 192 198 -  
 214. 199 205 206 212 TO 218 248 251 TO 257 265 271 272 278 279 285 TO 291 321 -  
 215. 324 TO 330 338 344 345 351 352 358 TO 364 394 397 TO 403 411 417 418 424 -  
 216. 425 431 TO 437 467 470 TO 476 484 490 491 497 498 504 TO 510 540 543 TO 549 -  
 217. 557 563 564 570 571 577 UNI GX 15.12  
 218. 1 TO 6 68 71 79 TO 84 105 111 119 125 133 139 TO 145 175 178 TO 184 192 198 -  
 219. 199 205 206 212 TO 218 248 251 TO 257 265 271 272 278 279 285 TO 291 321 -  
 220. 324 TO 330 338 344 345 351 352 358 TO 364 394 397 TO 403 411 417 418 424 -  
 221. 425 431 TO 437 467 470 TO 476 484 490 491 497 498 504 TO 510 540 543 TO 549 -  
 222. 557 563 564 570 571 577 UNI GY 15.12  
 223. 1 TO 6 68 71 79 TO 84 105 111 119 125 133 139 TO 145 175 178 TO 184 192 198 -  
 224. 199 205 206 212 TO 218 248 251 TO 257 265 271 272 278 279 285 TO 291 321 -  
 225. 324 TO 330 338 344 345 351 352 358 TO 364 394 397 TO 403 411 417 418 424 -  
 226. 425 431 TO 437 467 470 TO 476 484 490 491 497 498 504 TO 510 540 543 TO 549 -  
 227. 557 563 564 570 571 577 UNI GZ 15.12  
 228. FLOOR LOAD  
 229. YRANGE 0 21 FLOAD 5.8 XRANGE 0 29.5 ZRANGE 0 13.35 GX  
 230. YRANGE 0 21 FLOAD 5.8 XRANGE 0 29.5 ZRANGE 0 13.35 GY  
 231. YRANGE 0 21 FLOAD 5.8 XRANGE 0 29.5 ZRANGE 0 13.35 GZ  
 232. YRANGE 0 21 FLOAD 4 XRANGE 0 29.5 ZRANGE 0 13.35 GX  
 233. YRANGE 0 21 FLOAD 4 XRANGE 0 29.5 ZRANGE 0 13.35 GY  
 234. YRANGE 0 21 FLOAD 4 XRANGE 0 29.5 ZRANGE 0 13.35 GZ  
 235. GROUND MOTION X 1 1 9.806000  
 236. GROUND MOTION Z 2 1 9.806000  
 237. \*LOAD COMB 11 (STATIC + POSITIVE OF DYNAMIC)  
 238. \*1 1.0 2 1.0 3 1.0  
 239. \*LOAD COMB 12 (STATIC + NEGATIVE OF DYNAMIC)  
 240. \*1 1.0 2 1.0 3 -1.0  
 241. PERFORM ANALYSIS

STAAD SPACE

-- PAGE NO. 6

P R O B L E M   S T A T I S T I C S

-----  
NUMBER OF JOINTS            224    NUMBER OF MEMBERS        511  
NUMBER OF PLATES           0      NUMBER OF SOLIDS          0  
NUMBER OF SURFACES         0      NUMBER OF SUPPORTS        28

Using 64-bit analysis engine.

SOLVER USED IS THE OUT-OF-CORE BASIC SOLVER

ORIGINAL/FINAL BAND-WIDTH= 49/ 28/ 168 DOF  
TOTAL        PRIMARY LOAD CASES =     3, TOTAL DEGREES OF FREEDOM =    1176  
TOTAL LOAD COMBINATION CASES =     0 SO FAR.  
SIZE OF STIFFNESS MATRIX =     198 DOUBLE KILO-WORDS  
REQRD/AVAIL. DISK SPACE =     16.1/ 48861.3 MB

\*\*\*NOTE: MASSES DEFINED UNDER LOAD#        3 WILL FORM  
THE FINAL MASS MATRIX FOR DYNAMIC ANALYSIS.

EIGEN METHOD    : SUBSPACE

-----  
NUMBER OF MODES REQUESTED            =    30  
NUMBER OF EXISTING MASSES IN THE MODEL =    588  
NUMBER OF MODES THAT WILL BE USED    =    30

\*\*\* EIGENSOLUTION: SUBSPACE METHOD \*\*\*

STAAD SPACE

-- PAGE NO. 7

CALCULATED FREQUENCIES FOR LOAD CASE 3

| MODE | FREQUENCY(CYCLES/SEC) | PERIOD(SEC) | ACCURACY  |
|------|-----------------------|-------------|-----------|
| 1    | 1.002                 | 0.99757     | 1.791E-16 |
| 2    | 1.087                 | 0.91971     | 3.045E-16 |
| 3    | 1.131                 | 0.88455     | 0.000E+00 |
| 4    | 1.924                 | 0.51977     | 1.945E-16 |
| 5    | 2.057                 | 0.48620     | 0.000E+00 |
| 6    | 2.563                 | 0.39020     | 0.000E+00 |
| 7    | 2.995                 | 0.33385     | 1.123E-15 |
| 8    | 3.076                 | 0.32512     | 1.522E-16 |
| 9    | 3.278                 | 0.30510     | 4.021E-16 |
| 10   | 3.422                 | 0.29221     | 0.000E+00 |
| 11   | 3.502                 | 0.28557     | 3.523E-16 |
| 12   | 3.746                 | 0.26696     | 0.000E+00 |
| 13   | 3.965                 | 0.25220     | 1.832E-16 |
| 14   | 4.298                 | 0.23267     | 1.559E-16 |
| 15   | 4.314                 | 0.23183     | 3.095E-16 |
| 16   | 4.377                 | 0.22845     | 2.855E-15 |
| 17   | 4.718                 | 0.21193     | 6.467E-16 |
| 18   | 5.333                 | 0.18750     | 2.025E-16 |
| 19   | 5.380                 | 0.18588     | 3.184E-14 |
| 20   | 5.566                 | 0.17968     | 1.485E-12 |
| 21   | 5.832                 | 0.17146     | 1.673E-13 |
| 22   | 5.927                 | 0.16873     | 6.675E-13 |
| 23   | 6.231                 | 0.16048     | 2.258E-10 |
| 24   | 6.326                 | 0.15808     | 2.140E-13 |
| 25   | 6.363                 | 0.15717     | 3.709E-10 |
| 26   | 6.397                 | 0.15632     | 1.115E-09 |
| 27   | 6.593                 | 0.15167     | 1.207E-11 |
| 28   | 6.755                 | 0.14804     | 7.586E-09 |
| 29   | 7.099                 | 0.14086     | 4.489E-07 |
| 30   | 7.280                 | 0.13736     | 1.205E-07 |

The following Frequencies are estimates that were calculated. These are for information only and will not be used. Remaining values are either above the cut off mode/freq values or are of low accuracy. To use these frequencies, rerun with a higher cutoff mode (or mode + freq) value.

CALCULATED FREQUENCIES FOR LOAD CASE 3

| MODE | FREQUENCY(CYCLES/SEC) | PERIOD(SEC) | ACCURACY  |
|------|-----------------------|-------------|-----------|
| 31   | 7.770                 | 0.12871     | 5.877E-10 |



STAAD SPACE

-- PAGE NO. 8

CALCULATED FREQUENCIES FOR LOAD CASE 3

| MODE | FREQUENCY(CYCLES/SEC) | PERIOD(SEC) | ACCURACY  |
|------|-----------------------|-------------|-----------|
| 32   | 7.781                 | 0.12851     | 2.835E-06 |
| 33   | 7.994                 | 0.12510     | 3.314E-08 |

| MODE | MODAL WEIGHT (MODAL MASS TIMES g) IN KN |              |              | GENERALIZED WEIGHT |
|------|---|--------------|--------------|--------------------|
|      | X                                       | Y            | Z            |                    |
| 1    | 4.393456E+04                            | 4.477788E-04 | 2.823909E-03 | 2.624881E+04       |
| 2    | 2.616651E-02                            | 1.696310E-03 | 4.253945E+04 | 2.196378E+04       |
| 3    | 1.694206E+00                            | 4.216307E-04 | 2.940022E+02 | 1.207898E+04       |
| 4    | 1.080277E-05                            | 5.419254E-05 | 3.502036E+01 | 1.061509E+04       |
| 5    | 2.231742E-02                            | 1.154544E-04 | 2.163288E-02 | 1.890521E+04       |
| 6    | 2.895323E-04                            | 8.333211E-04 | 4.950516E-02 | 1.288106E+04       |
| 7    | 5.009322E-03                            | 1.922264E-04 | 6.303897E-07 | 2.117603E+04       |
| 8    | 5.226242E+03                            | 4.624638E-03 | 3.921081E-06 | 2.276884E+04       |
| 9    | 5.997593E-05                            | 1.518010E-03 | 8.401051E+00 | 1.435068E+04       |
| 10   | 2.019594E-03                            | 1.114409E-02 | 5.518197E+03 | 2.148180E+04       |
| 11   | 4.043703E-01                            | 1.454398E-03 | 2.674286E+01 | 2.614605E+04       |
| 12   | 2.272588E-01                            | 1.859533E-03 | 2.392859E-02 | 2.243453E+04       |
| 13   | 1.180115E-05                            | 5.987275E-04 | 1.402657E+02 | 1.060579E+04       |
| 14   | 4.572139E+01                            | 2.624980E-03 | 7.184260E-03 | 2.033325E+04       |
| 15   | 1.694784E-01                            | 8.861174E-03 | 1.332095E+00 | 9.826257E+03       |
| 16   | 1.749756E-05                            | 8.439970E-05 | 6.067123E-03 | 1.408948E+04       |
| 17   | 8.749197E-07                            | 1.682885E-02 | 3.992391E+01 | 1.653278E+04       |
| 18   | 1.908484E+03                            | 4.348200E-03 | 3.548795E-07 | 1.999455E+04       |
| 19   | 5.506569E-06                            | 7.782125E-04 | 3.155777E-01 | 1.185981E+04       |
| 20   | 1.876481E-04                            | 7.041190E-04 | 1.058043E-02 | 1.324976E+04       |
| 21   | 2.659550E-01                            | 4.394354E-04 | 7.808603E-07 | 1.753161E+04       |
| 22   | 1.207666E+00                            | 6.707230E-05 | 9.280289E-02 | 1.421897E+04       |
| 23   | 3.819683E-04                            | 7.988295E-03 | 2.026691E+03 | 1.858921E+04       |
| 24   | 1.074773E+02                            | 9.565444E-04 | 4.150215E-03 | 1.679893E+04       |
| 25   | 1.996438E-02                            | 1.691186E-03 | 1.178653E+00 | 1.267786E+04       |
| 26   | 2.492584E-07                            | 8.976651E-03 | 7.217180E+00 | 1.124337E+04       |
| 27   | 2.051554E-01                            | 5.071978E-03 | 3.886647E-05 | 1.563781E+04       |
| 28   | 2.575671E-06                            | 4.743532E-04 | 4.123751E+01 | 1.231606E+04       |
| 29   | 1.782793E-04                            | 2.731431E-02 | 8.285352E+00 | 6.594661E+03       |
| 30   | 3.337866E-12                            | 1.534310E-02 | 1.379742E+02 | 6.101120E+03       |

STAAD SPACE

-- PAGE NO. 9

MASS PARTICIPATION FACTORS

MASS PARTICIPATION FACTORS IN PERCENT

| MODE | X     | Y    | Z     | SUMM-X | SUMM-Y | SUMM-Z |
|------|-------|------|-------|--------|--------|--------|
| 1    | 82.45 | 0.00 | 0.00  | 82.448 | 0.000  | 0.000  |
| 2    | 0.00  | 0.00 | 79.83 | 82.448 | 0.000  | 79.830 |
| 3    | 0.00  | 0.00 | 0.55  | 82.451 | 0.000  | 80.381 |
| 4    | 0.00  | 0.00 | 0.07  | 82.451 | 0.000  | 80.447 |
| 5    | 0.00  | 0.00 | 0.00  | 82.451 | 0.000  | 80.447 |
| 6    | 0.00  | 0.00 | 0.00  | 82.451 | 0.000  | 80.447 |
| 7    | 0.00  | 0.00 | 0.00  | 82.451 | 0.000  | 80.447 |
| 8    | 9.81  | 0.00 | 0.00  | 92.258 | 0.000  | 80.447 |
| 9    | 0.00  | 0.00 | 0.02  | 92.258 | 0.000  | 80.463 |
| 10   | 0.00  | 0.00 | 10.36 | 92.258 | 0.000  | 90.818 |
| 11   | 0.00  | 0.00 | 0.05  | 92.259 | 0.000  | 90.869 |
| 12   | 0.00  | 0.00 | 0.00  | 92.260 | 0.000  | 90.869 |
| 13   | 0.00  | 0.00 | 0.26  | 92.260 | 0.000  | 91.132 |
| 14   | 0.09  | 0.00 | 0.00  | 92.345 | 0.000  | 91.132 |
| 15   | 0.00  | 0.00 | 0.00  | 92.346 | 0.000  | 91.134 |
| 16   | 0.00  | 0.00 | 0.00  | 92.346 | 0.000  | 91.134 |
| 17   | 0.00  | 0.00 | 0.07  | 92.346 | 0.000  | 91.209 |
| 18   | 3.58  | 0.00 | 0.00  | 95.927 | 0.000  | 91.209 |
| 19   | 0.00  | 0.00 | 0.00  | 95.927 | 0.000  | 91.210 |
| 20   | 0.00  | 0.00 | 0.00  | 95.927 | 0.000  | 91.210 |
| 21   | 0.00  | 0.00 | 0.00  | 95.928 | 0.000  | 91.210 |
| 22   | 0.00  | 0.00 | 0.00  | 95.930 | 0.000  | 91.210 |
| 23   | 0.00  | 0.00 | 3.80  | 95.930 | 0.000  | 95.013 |
| 24   | 0.20  | 0.00 | 0.00  | 96.132 | 0.000  | 95.013 |
| 25   | 0.00  | 0.00 | 0.00  | 96.132 | 0.000  | 95.016 |
| 26   | 0.00  | 0.00 | 0.01  | 96.132 | 0.000  | 95.029 |
| 27   | 0.00  | 0.00 | 0.00  | 96.132 | 0.000  | 95.029 |
| 28   | 0.00  | 0.00 | 0.08  | 96.132 | 0.000  | 95.106 |
| 29   | 0.00  | 0.00 | 0.02  | 96.132 | 0.000  | 95.122 |
| 30   | 0.00  | 0.00 | 0.26  | 96.132 | 0.000  | 95.381 |

A C T U A L MODAL D A M P I N G USED IN ANALYSIS

| MODE | DAMPING    |
|------|------------|
| 1    | 0.05000000 |
| 2    | 0.05000000 |
| 3    | 0.05000000 |
| 4    | 0.05000000 |
| 5    | 0.05000000 |
| 6    | 0.05000000 |
| 7    | 0.05000000 |
| 8    | 0.05000000 |
| 9    | 0.05000000 |
| 10   | 0.05000000 |
| 11   | 0.05000000 |
| 12   | 0.05000000 |
| 13   | 0.05000000 |

STAAD SPACE

-- PAGE NO. 10

| MODE | DAMPING    |
|------|------------|
| 17   | 0.05000000 |
| 18   | 0.05000000 |
| 19   | 0.05000000 |
| 20   | 0.05000000 |
| 21   | 0.05000000 |
| 22   | 0.05000000 |
| 23   | 0.05000000 |
| 24   | 0.05000000 |
| 25   | 0.05000000 |
| 26   | 0.05000000 |
| 27   | 0.05000000 |
| 28   | 0.05000000 |
| 29   | 0.05000000 |
| 30   | 0.05000000 |

TIME STEP USED IN TIME HISTORY ANALYSIS = 0.00139 SECONDS  
NUMBER OF MODES WHOSE CONTRIBUTION IS CONSIDERED = 30  
TIME DURATION OF TIME HISTORY ANALYSIS = 69.994 SECONDS  
NUMBER OF TIME STEPS IN THE SOLUTION PROCESS = 50396

242. PRINT STORY DRIFT

BASE SHEAR UNITS ARE -- KN METE

|                    |    |              |    |               |    |               |
|--------------------|----|--------------|----|---------------|----|---------------|
| MAXIMUM BASE SHEAR | X= | 4.864331E+03 | Y= | -1.576599E+00 | Z= | -5.053513E+03 |
| AT TIMES           |    | 19.531944    |    | 15.454167     |    | 14.105556     |

STORY DRIFT

STAAD SPACE

-- PAGE NO. 11

| STORY | HEIGHT<br>(METE) | LOAD | DRIFT(CM ) |         | ECCENTRICITY<br>(METE) | RATIO     |
|-------|------------------|------|------------|---------|------------------------|-----------|
|       |                  |      | X          | Z       |                        |           |
| BASE= | 0.00             |      |            |         |                        |           |
| 1     | 0.00             | 1    | 0.0000     | 0.0000  | 0.0000                 | L /999999 |
|       |                  | 2    | 0.0000     | 0.0000  | 0.0000                 | L /999999 |
|       |                  | 3    | 0.0000     | 0.0000  | 0.0000                 | L /999999 |
| 2     | 3.00             | 1    | 0.0001     | 0.0002  | 0.0000                 | L /999999 |
|       |                  | 2    | -0.0000    | -0.0000 | 0.0000                 | L /999999 |
|       |                  | 3    | -0.4834    | 0.3603  | 0.0000                 | L / 620   |
| 3     | 6.00             | 1    | 0.0005     | 0.0007  | 0.0000                 | L /999999 |
|       |                  | 2    | -0.0000    | -0.0000 | 0.0000                 | L /999999 |
|       |                  | 3    | -1.1806    | 0.9485  | 0.0000                 | L / 508   |
| 4     | 9.00             | 1    | 0.0010     | 0.0016  | 0.0000                 | L /571652 |
|       |                  | 2    | -0.0000    | -0.0000 | 0.0000                 | L /999999 |
|       |                  | 3    | -1.8316    | 1.5212  | 0.0000                 | L / 491   |
| 5     | 12.00            | 1    | 0.0016     | 0.0026  | 0.0000                 | L /454889 |
|       |                  | 2    | -0.0000    | -0.0000 | 0.0000                 | L /999999 |
|       |                  | 3    | -2.3811    | 2.0100  | 0.0000                 | L / 504   |
| 6     | 15.00            | 1    | 0.0024     | 0.0039  | 0.0000                 | L /388280 |
|       |                  | 2    | -0.0000    | -0.0000 | 0.0000                 | L /999999 |

STAAD SPACE -- PAGE NO. 12

|   |       |   |         |         |        |           |
|---|-------|---|---------|---------|--------|-----------|
|   |       | 3 | 2.8193  | 2.3958  | 0.0000 | L / 532   |
| 7 | 18.00 | 1 | 0.0033  | 0.0052  | 0.0000 | L /347159 |
|   |       | 2 | -0.0000 | -0.0000 | 0.0000 | L /999999 |
|   |       | 3 | 3.1291  | 2.6733  | 0.0000 | L / 575   |
| 8 | 21.00 | 1 | 0.0042  | 0.0065  | 0.0000 | L /324632 |
|   |       | 2 | -0.0000 | -0.0000 | 0.0000 | L /999999 |
|   |       | 3 | 3.2961  | 2.8461  | 0.0000 | L / 637   |

243. FINISH

\*\*\*\*\* END OF THE STAAD.Pro RUN \*\*\*\*\*

\*\*\* DATE= APR 2,2020 TIME= 19:13: 3 \*\*\*

STAAD SPACE

-- PAGE NO. 13

```
*****  
* For technical assistance on STAAD.Pro, please visit *  
* http://www.bentley.com/en/support/ *  
* *  
* Details about additional assistance from *  
* Bentley and Partners can be found at program menu *  
* Help->Technical Support *  
* *  
* Copyright (c) 1997-2017 Bentley Systems, Inc. *  
* http://www.bentley.com *  
*****
```

## **APPENDIX B**

### **MAXIMUM ROOF DISPLACEMENT UNDER AS-RECORDED AND MD GROUND**

#### **MOTIONS**

The numerical values of the maximum response (lateral displacement) and response (lateral displacement) in the as-recorded orientation of ground motions at center of mass of roof level for all four building models is shown here. Chapter 4 describes these values as Maximum direction and as-recorded. All values are in centimeters.

**Table 2.** Maximum roof displacement under as-recorded and MD ground motions.

| GM No. | (BM1)       |                   |             |                   | (BM2)       |                   |             |                   |
|--------|-------------|-------------------|-------------|-------------------|-------------|-------------------|-------------|-------------------|
|        | X           |                   | Z           |                   | X           |                   | Z           |                   |
|        | As-recorded | Maximum Direction | As-recorded | Maximum Direction | As-recorded | Maximum Direction | As-recorded | Maximum Direction |
| 1      | 0.0637      | 0.1538            | 0.1347      | 0.1544            | 0.1109      | 0.1406            | 0.0235      | 0.1487            |
| 2      | 0.1275      | 0.149             | 0.0025      | 0.1326            | 0.092       | 0.1513            | 0.1471      | 0.1544            |
| 3      | 0.0923      | 0.1326            | 0.1118      | 0.1286            | 0.1067      | 0.1225            | 0.0264      | 0.1379            |
| 4      | 0.0069      | 0.0291            | 0.0179      | 0.0315            | 0.039       | 0.0469            | 0.0217      | 0.0473            |
| 5      | 0.0554      | 0.2205            | 0.1119      | 0.1946            | 0.1612      | 0.1967            | 0.1966      | 0.2048            |
| 6      | 0.1816      | 0.2844            | 0.2331      | 0.2589            | 0.1764      | 0.2325            | 0.2241      | 0.236             |
| 7      | 0.0629      | 0.3113            | 0.1084      | 0.3072            | 0.272       | 0.298             | 0.1978      | 0.322             |
| 8      | 0.0565      | 0.0573            | 0.0332      | 0.0577            | 0.0619      | 0.0624            | 0.0178      | 0.0647            |
| 9      | 0.2313      | 0.3723            | 0.2558      | 0.3438            | 0.2933      | 0.4442            | 0.0791      | 0.4885            |
| 10     | 0.2096      | 0.217             | 0.1111      | 0.1932            | 0.1505      | 0.1563            | 0.0117      | 0.1613            |
| 11     | 0.0557      | 0.1554            | 0.0986      | 0.1326            | 0.1012      | 0.125             | 0.0943      | 0.1434            |
| 12     | 0.053       | 0.0901            | 0.0403      | 0.083             | 0.0466      | 0.0729            | 0.0779      | 0.078             |
| 13     | 0.0679      | 0.0686            | 0.0403      | 0.0714            | 0.0644      | 0.0645            | 0.032       | 0.0654            |
| 14     | 0.1624      | 0.1654            | 0.1337      | 0.1692            | 0.1787      | 0.1799            | 0.0893      | 0.1829            |
| 15     | 0.149       | 0.7459            | 0.5899      | 0.6974            | 0.196       | 0.7231            | 0.1911      | 0.7429            |
| 16     | 0.2653      | 0.286             | 0.2576      | 0.2773            | 0.2755      | 0.3305            | 0.2459      | 0.3351            |
| 17     | 0.0614      | 0.1321            | 0.1256      | 0.1262            | 0.0343      | 0.1366            | 0.1387      | 0.1394            |
| 18     | 0.0342      | 0.0357            | 0.0298      | 0.037             | 0.006       | 0.0386            | 0.454       | 0.0462            |
| 19     | 0.0104      | 0.0741            | 0.0216      | 0.0693            | 0.0534      | 0.0772            | 0.0721      | 0.0721            |
| 20     | 0.0907      | 0.0941            | 0.0401      | 0.1064            | 0.0736      | 0.0958            | 0.0535      | 0.1007            |
| 21     | 0.0595      | 0.627             | 0.0442      | 0.061             | 0.0582      | 0.0614            | 0.0403      | 0.0628            |
| 22     | 0.2083      | 0.2093            | 0.1062      | 0.1959            | 0.1776      | 0.1924            | 0.1122      | 0.1946            |
| 23     | 0.019       | 0.0196            | 0.0135      | 0.0178            | 0.0027      | 0.0135            | 0.0007      | 0.0138            |
| 24     | 0.1506      | 0.1635            | 0.1479      | 0.1484            | 0.1486      | 0.1508            | 0.1349      | 0.1508            |
| 25     | 0.0874      | 0.1287            | 0.0722      | 0.1269            | 0.0366      | 0.112             | 0.1117      | 0.115             |



**Table 2.** Maximum roof displacement under as-recorded and MD ground motions. (continued)

| GM No. | (BM3)       |                   |             |                   | (BM4)       |                   |             |                   |
|--------|-------------|-------------------|-------------|-------------------|-------------|-------------------|-------------|-------------------|
|        | X           |                   | Z           |                   | X           |                   | Z           |                   |
|        | As-recorded | Maximum Direction | As-recorded | Maximum Direction | As-recorded | Maximum Direction | As-recorded | Maximum Direction |
| 1      | 0.9632      | 1.3147            | 1.1028      | 1.2194            | 0.9536      | 1.2975            | 1.2769      | 1.3095            |
| 2      | 3.2269      | 3.7369            | 3.5245      | 3.8429            | 0.5606      | 3.6857            | 3.7287      | 3.7287            |
| 3      | 3.2858      | 3.7354            | 2.8137      | 2.8957            | 2.1976      | 3.707             | 3.7075      | 3.7413            |
| 4      | 0.2625      | 0.3292            | 0.3592      | 0.3592            | 0.1916      | 0.3254            | 0.1086      | 0.3284            |
| 5      | 0.3539      | 0.948             | 0.928       | 0.98              | 0.27        | 0.9571            | 0.9118      | 0.9569            |
| 6      | 0.9845      | 1.1507            | 0.8934      | 1.209             | 0.4229      | 1.1269            | 0.9119      | 1.1583            |
| 7      | 1.5874      | 1.5874            | 1.3717      | 1.3717            | 1.5366      | 1.5366            | 1.0733      | 1.556             |
| 8      | 0.8291      | 0.8973            | 0.7789      | 0.7789            | 0.8159      | 0.8793            | 0.5303      | 0.8961            |
| 9      | 0.2526      | 0.9022            | 0.9261      | 0.9265            | 0.2377      | 0.8154            | 0.8064      | 0.8202            |
| 10     | 4.1036      | 4.3656            | 3.5084      | 5.0648            | 2.7934      | 4.188             | 4.0028      | 4.313             |
| 11     | 1.9338      | 2.4013            | 1.1187      | 2.1334            | 0.5301      | 1.8371            | 1.3685      | 2.3819            |
| 12     | 1.2942      | 2.0457            | 1.2396      | 1.5656            | 1.225       | 2.0078            | 2.0375      | 2.0659            |
| 13     | 0.6986      | 1.054             | 1.043       | 1.0448            | 0.6865      | 0.912             | 0.7419      | 1.0153            |
| 14     | 3.3377      | 6.9696            | 5.0619      | 5.48              | 3.1679      | 6.9331            | 6.9483      | 6.9995            |
| 15     | 14.0468     | 15.6969           | 14.5335     | 17.9831           | 5.662       | 15.2505           | 13.101      | 15.6833           |
| 16     | 14.4732     | 15.1693           | 6.2151      | 9.1014            | 14.5226     | 15.1213           | 6.1107      | 15.3672           |
| 17     | 0.4081      | 0.7185            | 0.6466      | 0.8201            | 0.4169      | 0.6118            | 0.5795      | 0.6989            |
| 18     | 0.1718      | 0.2699            | 0.2669      | 0.268             | 0.1756      | 0.2564            | 0.1917      | 0.2617            |
| 19     | 1.2066      | 1.482             | 0.7749      | 1.1164            | 1.0145      | 1.4986            | 0.2914      | 1.5051            |
| 20     | 0.8137      | 0.816             | 0.2793      | 0.7445            | 0.8232      | 0.8279            | 0.6759      | 0.8297            |
| 21     | 3.2176      | 3.6043            | 1.9862      | 3.0391            | 3.1901      | 3.5829            | 2.2036      | 3.5985            |
| 22     | 8.5132      | 8.6029            | 3.5529      | 9.0019            | 8.6731      | 8.7443            | 3.929       | 8.6232            |
| 23     | 0.6546      | 0.6798            | 0.3708      | 0.5948            | 0.6311      | 0.6516            | 0.3513      | 0.6697            |
| 24     | 2.7445      | 2.7609            | 1.711       | 2.2941            | 2.7373      | 2.7495            | 1.91        | 2.8017            |
| 25     | 1.2139      | 1.8323            | 0.1754      | 1.4035            | 0.6484      | 1.8373            | 1.8739      | 1.8936            |

VITA

Graduate School  
Southern Illinois University

Amanullah Parsa

amanullah.parsa@siu.edu

Osmania University  
Bachelor of Engineering, Civil Engineering, May 2015

Thesis Paper Title:

EFFECT OF BUILDING ORIENTATION ON STRUCTURAL RESPONSE OF  
REINFORCED CONCRETE MOMENT RESISTING FRAME STRUCTURES

Major Professor: Dr. Jale Tezcan